Copy 6
RM L53A09c

NACA

RESEARCH MEMORANDUM

LIFT AND DRAG CHARACTERISTICS OF THE BELL X-5 RESEARCH AIRPLANE AT 59° SWEEPBACK FOR MACH NUMBERS FROM 0.60 TO 1.03

By Donald R. Bellman

Langley Aeronautical Laboratory
Langley Field, Va.

NATIONAL ADVISORY COMMITTEE FOR AERONAUTICS

WASHINGTON

February 17, 1953

NATIONAL ADVISORY COMMITTEE FOR AERONAUTICS

RESEARCH MEMORANDUM

LIFT AND DRAG CHARACTERISTICS OF THE BELL X-5 RESEARCH AIRPLANE AT 59° SWEEPBACK FOR MACH NUMBERS FROM 0.60 TO 1.03

By Donald R. Bellman

SUMMARY

The National Advisory Committee for Aeronautics is investigating the flight characteristics of the Bell X-5 research airplane which has sweepback that can be varied from 20° to 59° in flight. Lift and drag data have been obtained for the 59° sweep configuration for the Mach number range from 0.60 to 1.03 and from zero to almost maximum lift. A brief comparison between the 20° and 59° configuration is also made.

Near zero lift coefficient and within the Mach number range tested, the lift-curve slopes ranged between 0.04 and 0.05 deg^{-1}. At zero lift the drag rise occurred at a Mach number of about 0.93. At a lift coefficient of 0.20 the maximum rate of rise in drag coefficient occurred at a Mach number of 0.96 with the drag rising only slightly at a Mach number of 1.03 where it had a value of 0.073. The induced drag factor $dC_D/dC_L{}^2$ was of the order of 0.33.

For level flight at an altitude of 42,000 feet the 20° configuration had considerably less drag force than the 59° configuration for Mach numbers below 0.81, whereas above a Mach number of 0.82 the reverse was true. At an altitude of 42,000 feet and a Mach number of 0.74 the total drag force for lift coefficients between 0.4 and 0.7 was at least twice as great for the 59° sweep configuration as that for the 20° sweep configuration.

INTRODUCTION

The NACA High Speed Flight Research Station, Edwards, Calif., is performing a flight evaluation of the Bell X-5 research airplane. The investigation is to cover the lift and speed ranges of which the airplane is capable at each of several different sweep angles between the limits of 20° and 59°. This paper presents lift and drag data obtained with the wings swept to 59° and covers the Mach number range from 0.60 to 1.03. It also includes a brief comparison of the drag between the 20° and 59° wing-sweep configurations. The flights from which the data were obtained were made in the period from January through August 1952.

The data presented in this report were taken during flights of the airplane for which the instrumentation was intended primarily for stability, control, and loads measurements. It was not possible, because of instrument space limitations, to measure all the usual quantities needed for precise determination of lift, drag, and angle of attack. Nevertheless, the results presented herein are believed to give a reasonably accurate picture of the performance of this configuration.

SYMBOLS

C_D	drag coefficient
C_L	lift coefficient
C_N	normal-force coefficient
C_X	longitudinal-force coefficient
F_n	net thrust, lb
M	Mach number
N	engine speed, rpm
S	wing area, sq ft
T	atmospheric temperature, degrees Rankine
W	airplane weight, lb
a_X	recorded longitudinal acceleration, g units
p	atmospheric pressure, lb/sq ft
q	dynamic pressure, lb/sq ft
α	angle of attack, deg

δ_c altitude normalizing factor, $\delta_c = \frac{p\left(1 + 0.2M^2\right)^{3.5}}{2116}$

θ_c temperature normalizing factor, $\theta_c = \frac{T\left(1 + 0.2M^2\right)}{518.4}$

Λ wing sweep angle, measured at the quarter chord, deg

D total drag force, lb

n normal acceleration, g units

a lift-curve slope, $\frac{dC_L}{d\alpha}$, deg^{-1}

$\frac{dC_D}{d{C_L}^2}$ induced drag factor

M.A.C. mean aerodynamic chord, ft

c chord, ft

AIRPLANE

The X-5 research airplane used by the NACA is one of two built by the Bell Aircraft Company, and is a single-place turbojet-powered airplane having a wing sweep angle that can be varied in flight. The sweep of this particular model can be varied from 20.2° to 58.7° and simultaneously the wings translate to maintain essentially a constant relationship between the center of gravity and the aerodynamic center. Total translation amounts to 27 inches. The wing slats were locked in the fully retracted position for all tests reported in this paper.

Table I presents the general physical characteristics of the airplane. Figure 1 shows photographs of the 59° and 20° sweep configuration and figure 2 is a three-view sketch of the airplane in the 59° configuration. Plan views of the wing at the 59° and 20° sweep angles are shown in figure 3. The extensive modifications at the root necessary to achieve the variable sweep are indicated and it can be seen that the 20° configuration deviates more from the basic wing shape than does the 59° configuration. Section A-A shows how the leading edge of the wing root has been extended and the trailing edge shortened giving the effect of a blunt trailing edge on a section having the maximum thickness quite far aft.

The streamwise wing thickness in percent chord decreases from root to tip and also varies with the sweep angle. At 20° sweep it is 12.35 at the root, 10.04 at the mean aerodynamic chord, and 7.99 at the tip. At 59° sweep the thicknesses are 6.94, 5.99, and 4.68, respectively. These figures are based on the actual chords of the modified wing and at the root of the 20° sweep configuration the flat plate is included in the chord length.

INSTRUMENTATION

Altitude and airspeed were determined by means of an NACA airspeed head mounted on the nose boom and recorded on standard NACA flight instruments. The airspeed installation was calibrated in flight by means of radar-phototheodolite. Angle of attack was measured by means of a vane attached to an arm projecting from the nose boom. The vane is approximately 50 inches ahead of the nose fairing and 7 inches to the left of the center line of the boom. Accelerations were measured by a standard NACA 3-component accelerometer and in addition longitudinal accelerations were also measured by means of a sensitive longitudinal accelerometer mounted in the instrument compartment in the aft fuselage. A recording tachometer was used to measure the engine speed for use in the thrust computations.

CALCULATIONS

Instrumentation for measuring thrust in flight was not available for most of these tests; therefore, thrust was calculated from the corrected recorded pressure altitude, flight speed, engine speed, and NACA standard atmospheric temperature. The calculations were based on wind tunnel and thrust stand tests of the same model engine (refs. 1 and 2) correlated with the measured ground level thrust of the engine installed in the airplane. Figure 4 shows the normalized thrust obtained by running the airplane on the Edwards Air Force Base thrust stand. Figure 5 shows the factors for correcting the thrust for flight Mach number which were obtained from data presented in references 1 and 2. The true thrust is merely the normalized thrust taken from figure 4 multiplied by the Mach number correction factor from figure 5 and by the altitude normalizing factor δ_c.

The lift and drag coefficients were computed using the following formulas:

$$C_N = \frac{Wn}{qS}$$

$$C_X = \frac{F_n - Wa_X}{qS}$$

$$C_L = C_N \cos \alpha - C_X \sin \alpha$$

$$C_D = C_X \cos \alpha + C_N \sin \alpha$$

ACCURACY

The accuracy of the values of drag coefficient is primarily determined by the accuracy of thrust, although normal acceleration, longitudinal acceleration, and angle of attack also have considerable effect. On a few flights the air inlet duct and the tail pipe were instrumented for thrust measurement and the results compared with those from the method used for this paper. A check of about 200 data points which covered the Mach number range from 0.69 to 0.92 and the altitude range from 30,000 to 35,000 feet, showed that the measured values of thrust averaged about 200 pounds lower than the calculated values of thrust which were used for the data of this paper. At an altitude of 35,000 feet and a Mach number of 0.6, this variation in thrust would cause a variation in drag coefficient of 0.009. At the same altitude and a Mach number of 1.0 the variation in drag coefficient would be 0.003.

The position of the angle-of-attack vane can be measured within $\pm 0.2^{\circ}$, but a calibration in an air stream was not made so the error caused by the upwash field ahead of the airplane could not be determined. The upwash field caused by the wing can be calculated and assuming the wing extends to the center of the fuselage the calculations show that there would be a 6-percent error in angle of attack at a Mach number of 0.6. This error would decrease with increasing Mach number. The effect of upwash caused by the fuselage, the effect of the boom, and the effect of pitching velocity were not taken into account.

The airspeed calibration, the method of which is described in reference 3, is believed to give Mach numbers that are accurate within ±0.01. The normal accelerations were accurate within ±0.05g, and the longitudinal accelerations were accurate within ±0.01g. The take-off weight of the airplane was known within 100 pounds and corrections were made for fuel consumed in flight.

TESTS, RESULTS, AND DISCUSSION

The flight maneuvers used to determine the lift and drag characteristics consisted of speed runs, pull-ups, push-downs, and accelerated turns. The maneuvers covered the speed range from a Mach number of 0.60 to a Mach number of 1.03, and the lift range from zero to points well above the boundary for reduction of longitudinal stability. The altitude range of the maneuvers varied from 30,000 to 43,000 feet.

59° Sweep Configuration

The variation of lift coefficient and drag coefficient with angle of attack is shown in figure 6 for various constant Mach numbers from 0.60 to 0.96. The data shown are for a range of Mach numbers on either side of the Mach number given in the figure of from 0.008 for the low speeds to 0.002 for Mach numbers above 0.91. The data for each curve were taken from several maneuvers and are presented independent of pitching acceleration which may produce some of the scatter.

At each Mach number the slope of the lift curve seemed to increase from its value at low lift coefficients to some higher value occurring at a lift coefficient between 0.3 and 0.5 before decreasing as the maximum lift is approached. This effect is more noticeable in the plots of single maneuvers than in the composite data of figure 6. The lift-curve slopes for 25 pull-ups were measured over the lift-coefficient ranges from 0 to 0.3 and from 0.3 to 0.5 and are presented in figure 7. For the Mach number range tested the lift-curve slopes varied from 0.040 deg^{-1} to 0.050 deg^{-1} for the lower lift-coefficient range and from 0.050 deg^{-1} to 0.058 deg^{-1} for the higher lift-coefficient range.

Conventional drag polars are presented in figure 8 for selected Mach numbers from 0.60 to 1.03. Data were taken from similar Mach number bands as for figure 6. Figure 9 is a cross plot of the data of figure 8 and shows the variation of drag coefficient with Mach number for selected lift coefficients. A minimum zero-lift drag coefficient of 0.019 occurred at a Mach number of about 0.80. The Mach number at which the drag rise occurred varied from about 0.93 at zero lift to about 0.76 at a lift coefficient of 0.7. The drag coefficient for a lift coefficient of 0.20 has a minimum point of 0.027 around a Mach number of 0.84. The drag rise occurs at a Mach number of about 0.93 and the most rapid rate of increase is reached at a Mach number of about 0.96. Above this Mach number the rate of increase continually decreases. At the maximum Mach number $M = 1.03$, the drag coefficient has a value of 0.073 at $C_L = 0.20$.

The induced drag factor $\frac{dC_D}{dC_L^2}$ has been obtained from plots of C_D against C_L^2 for each selected Mach number. A typical curve is presented in figure 10 and it can be seen that the slope is essentially constant for the C_L^2 range from 0.05 to 0.45. Below this range the slope becomes less and above this range the slope becomes greater. The variation with Mach number of the induced drag factor as determined in the above manner is shown in figure 11. The C_L^2 range for the straight portion of the curve varies slightly and at the higher Mach numbers only the lower portions of the curves were obtained. The lift-curve range corresponds roughly to the high range of figure 7. The induced drag factor has a value of about 0.33 from a Mach number of 0.60 to 0.84 where it then increases to about 0.39 as the Mach number increases to 0.95.

Comparison of the 20° and 59° Sweep Configurations

A small amount of data for the 20° sweep configuration presently available makes possible a brief comparison between the 20° and 59° configurations. It should be emphasized, however, that in addition to a change in wing sweep from 59° to 20° there is also a change in wing area from 184.3 square feet to 166.9 square feet, a change in aspect ratio from 2.16 to 6.09, and as previously mentioned a change in the ratio of wing thickness to chord and also the wing root profile becomes completely different.

Drag results of a level run with the 20° sweep configuration are presented in figure 12. The run was made at an altitude of approximately 42,000 feet and Mach number varied from 0.64 to 0.84. For comparison the drag for the 59° sweep configuration for the same test altitudes and Mach numbers was calculated from data presented in figure 8 and is shown as a solid line on figure 12. The plot of the difference between the thrust and drag forces shows that, at the test altitude, level flight at Mach numbers between 0.64 and 0.79 cannot be maintained with the 59° configuration, whereas, it can be maintained with the 20° configuration. Above a Mach number of 0.82, the reverse is true. Figure 12 shows the desirability of climbing to high altitudes using 20° sweep and then changing to 59° sweep for high-speed flight.

Figure 13 presents data from two pull-ups; one with 20° sweep and the other with 59° sweep. Both were made at a Mach number of 0.74 and an altitude of 42,000 feet. It can be seen from figure 13 that at this Mach number the total drag force for the 59° configuration is at least twice that for the 20° configuration for lift coefficients below maximum lift. The maximum lift coefficient for the 20° configuration is about 0.1 below that for the 59° configuration.

CONCLUSIONS

The following conclusions were drawn from the results of lift and drag data obtained from flight tests of the Bell X-5 airplane with 59° sweepback:

1. As the Mach number varied from 0.60 to 0.96 the lift-curve slope for lift coefficients between 0 and 0.3 varied from 0.04 to 0.05 deg^{-1}.

2. The minimum zero-lift drag coefficient is 0.019 and occurred at a Mach number of 0.80.

3. For a lift coefficient of 0.20 the most rapid rate of increase in drag coefficient with Mach number occurred at a Mach number of about 0.96. At a Mach number of 1.03 the drag coefficient reached a value of 0.073 and was increasing only slightly.

4. At zero lift the drag rise occurred at a Mach number of about 0.93.

5. The induced drag factor $\frac{dC_D}{d{C_L}^2}$ had a value of about 0.33 for Mach numbers below 0.84 and increased to a value of 0.39 at a Mach number of 0.94.

The comparison of the 59° and 20° sweep configurations resulted in the following conclusions:

1. At an altitude of about 42,000 feet the drag force for the 20° sweep configuration in unaccelerated flight was considerably less than that for the 59° sweep configuration for flight speeds below a Mach number of 0.81; above a Mach number of 0.82 the reverse is true.

2. At an altitude of 42,000 feet and at a Mach number of 0.74 the total drag force for the 59° configuration was more than twice that for the 20° configuration at any given lift coefficient below maximum lift.

Langley Aeronautical Laboratory,
National Advisory Committee for Aeronautics,
Langley Field, Va.

REFERENCES

1. Vincent, K. R., and Gale, B. M.: Altitude Performance of J35-A-17 Turbojet Engine in an Altitude Chamber. NACA RM E50I15, 1951.

2. Cochran, John T., and Searcy, Dallas T.: Engine Thrust and Airflow Calibration for the X-5 Aircraft. MR No. MCRFT-2340, Air Materiel Command, U. S. Air Force, Mar. 29, 1951.

3. Rogers, John T., and Dunn, Angel H.: Preliminary Results of Horizontal-Tail Load Measurements of the Bell X-5 Research Airplane. NACA RM L52G14, 1952.

TABLE I

PHYSICAL CHARACTERISTICS OF BELL X-5 AIRPLANE

Airplane:		
Weight, lb:		
Full fuel		9960
Less fuel		7850
Power plant:		
Axial-flow turbojet engine		J-35-A-17
Guaranteed rated thrust at 7800 rpm and static sea-level conditions, lb		4900
Center-of-gravity position, percent M.A.C.:		
Full fuel		45.6
Less fuel		46.2
Over-all height, ft		12.2
Over-all length, ft		33.6
Wing:		
Airfoil section (perpendicular to 38.02-percent-chord line):		
Pivot point		NACA $64_{(10)}$A011
Tip		NACA $64_{(08)}$A008.28
Sweep angle at 0.25 chord, deg	20	59
Area, sq ft	166.9	184.3
Span, ft	31.9	20.0
Span between equivalent tips, ft	30.9	19.2
Aspect ratio	6.09	2.16
Taper ratio	0.435	0.4095
Mean aerodynamic chord, ft	5.61	10.05
Location of leading edge of mean aerodynmic chord, fuselage station	139.9	100.2
Incidence root chord, deg	0	0
Dihedral, deg	0	0
Geometric twist, deg	0	0
Wing flaps (split):		
Area, sq ft		15.9
Span, parallel to hinge center line, ft		6.53
Chord, parallel to line of symmetry at 20° sweepback, in.:		
Root		30.8
Tip		19.2
Travel, deg		60

NACA

TABLE I.- Continued

PHYSICAL CHARACTERISTICS OF BELL X-5 AIRPLANE

Slats (leading edge divided):	
Area, sq ft	14.6
Span, parallel to leading edge, ft	10.3
Chord, perpendicular to leading edge, in.:	
Root	11.1
Tip	6.6
Travel, percent wing chord:	
Forward	10
Down	5
Aileron (45 percent internal seal pressure-balance):	
Area (each aileron behind hinge line), sq ft	3.62
Span parallel to hinge center line, ft	5.15
Travel, deg	±15
Chord, percent wing chord	19.7
Moment area rearward of hinge line (total), in.^{3}	4380
Horizontal tail:	
Airfoil section (parallel to fuselage center line)	NACA 65A006
Area, sq ft	31.5
Span, ft	9.56
Aspect ratio	2.9
Sweep angle at 0.25 percent chord, deg	45
Mean aerodynamic chord, in.	42.8
Position of 0.25 mean aerodynamic chord, fuselage station	355.6
Stabilizer travel, (power actuated), deg:	
Leading edge up	4.5
Leading edge down	7.5
Elevator (20.8 percent overhang balance, 31.5 percent span):	
Area rearward of hinge line, sq ft	6.9
Travel from stabilizer, deg:	
Up	25
Down	20
Chord, percent horizontal tail chord	30
Moment area rearward of hinge line (total), in.^{3}	4200

NACA

TABLE I.- Concluded

PHYSICAL CHARACTERISTICS OF BELL X-5 AIRPLANE

Vertical tail:	
Airfoil section (parallel to rear fuselage center line)	NACA 65A006
Area, sq ft	29.5
Span, perpendicular to rear fuselage center line, ft	6.25
Aspect ratio	1.32
Sweep angle of leading edge, deg	43
Fin:	
Area, sq ft	24.8
Rudder (23.1 percent overhang balance, 26.3 percent span):	
Area rearward of hinge line, sq ft	4.7
Span, ft	4.43
Travel, deg	±35
Chord, percent horizontal tail chord	22.7
Moment area rearward of hinge line, $in.^3$	3585

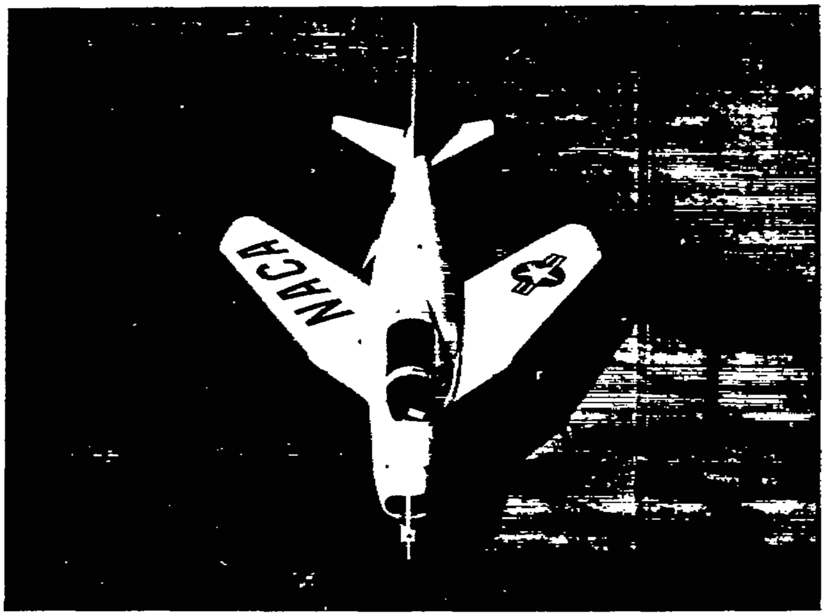

(a) $\Lambda = 59^{\circ}$. NACA LE-811

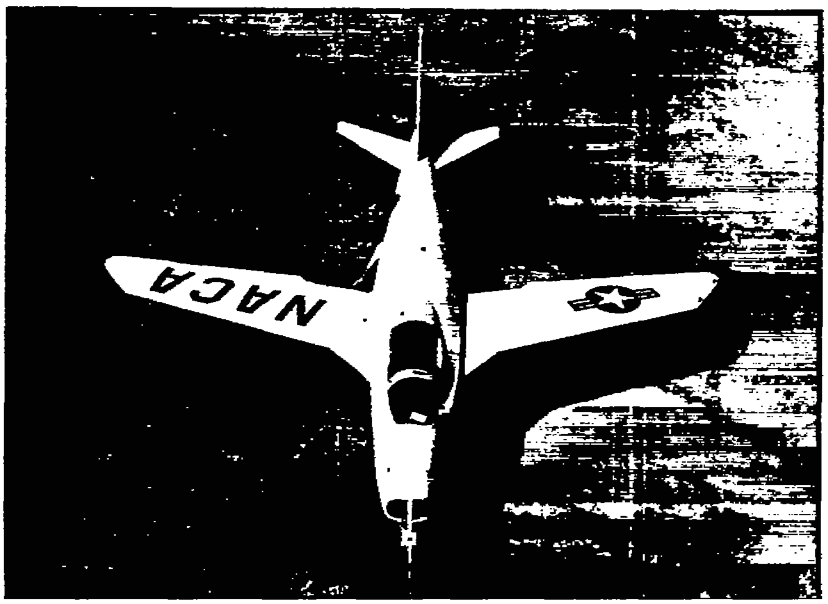

(b) $\Lambda = 20^{\circ}$. NACA LE-813

Figure 1.- Photographs of the Bell X-5 research airplane.

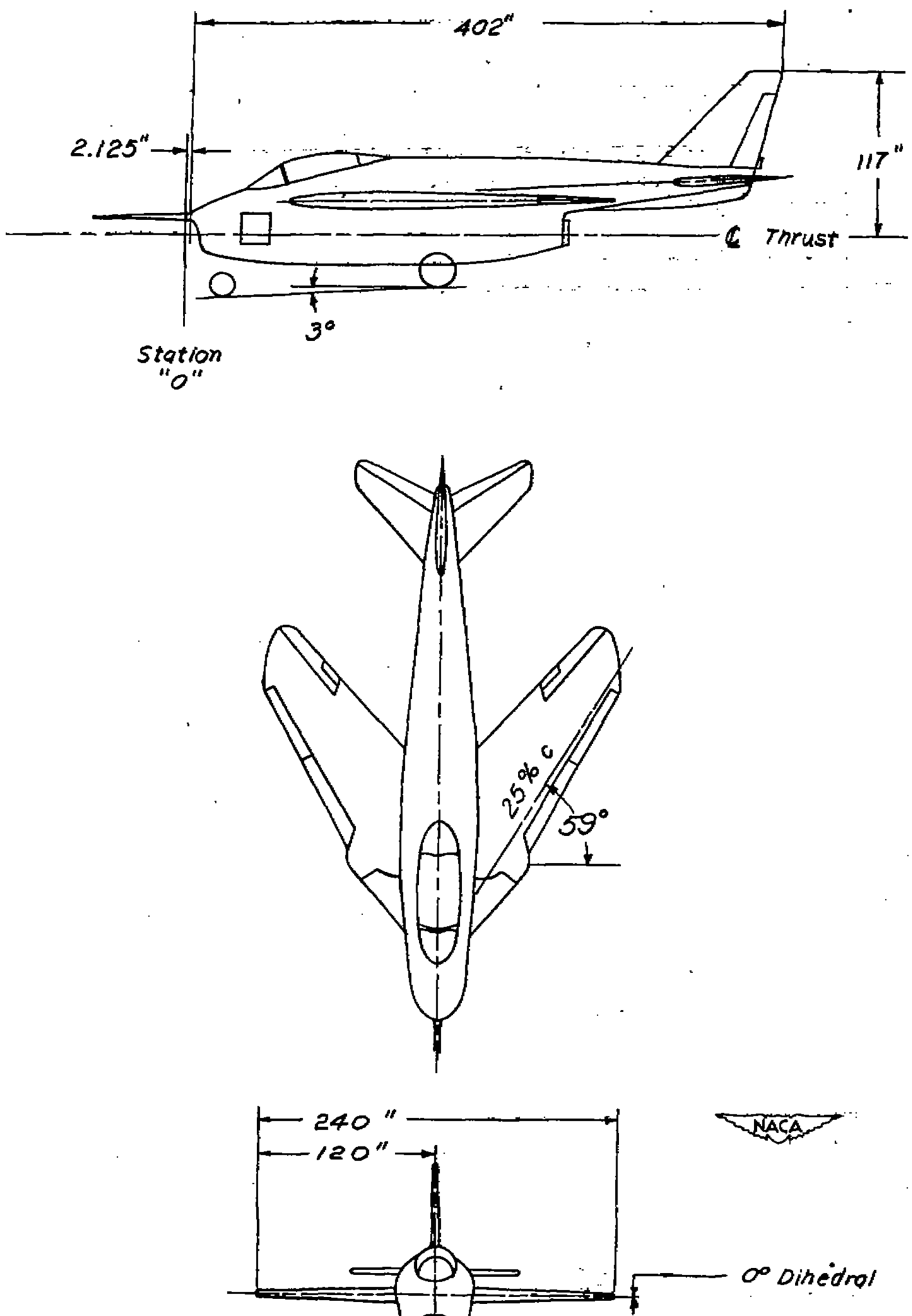

Figure 2.- Three-view drawing of Bell X-5 research airplane at 59° sweepback.

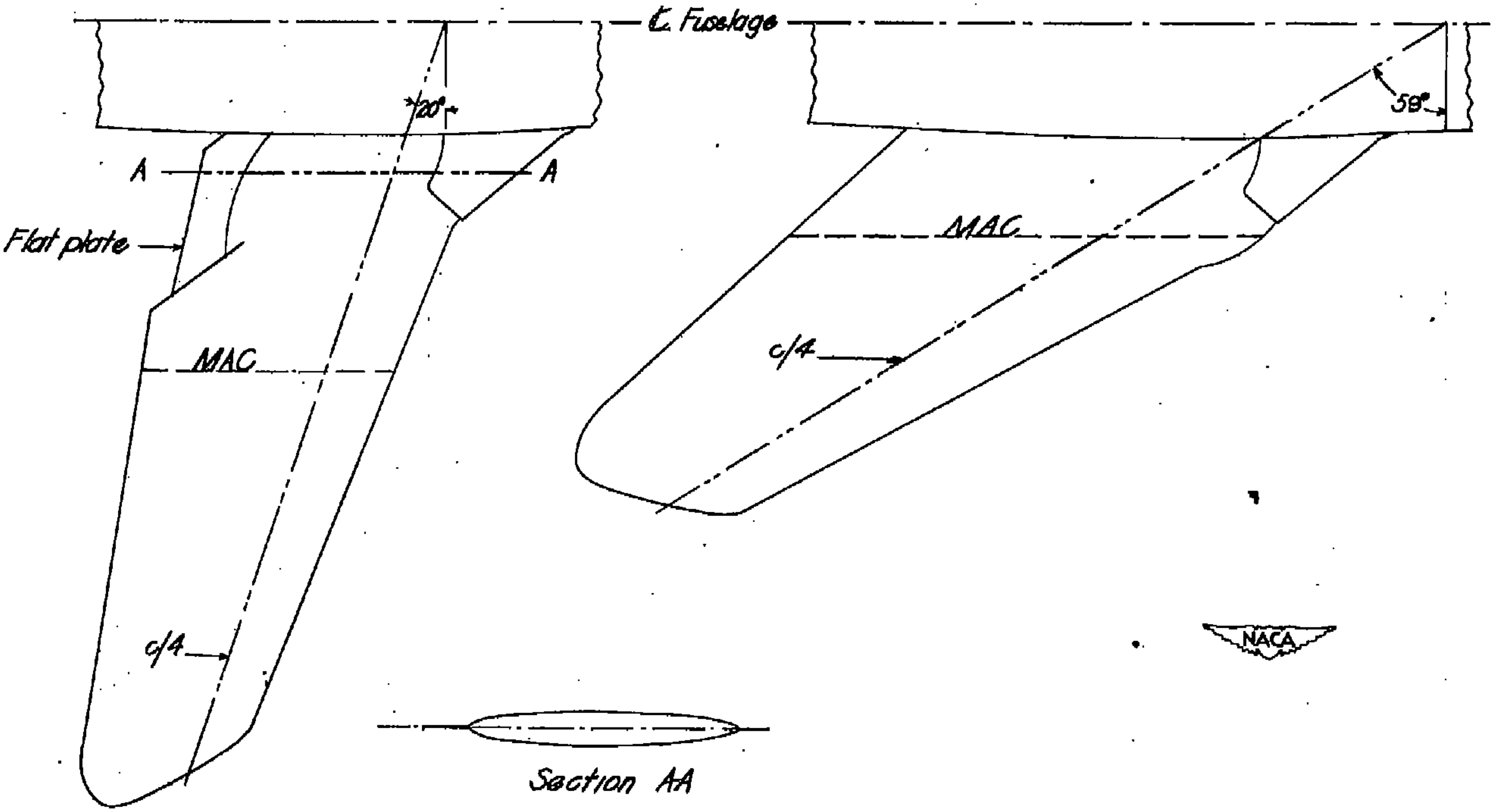

Figure 3.- Sketch showing differences in wing plan form between the 20° and 59° sweptback configurations.

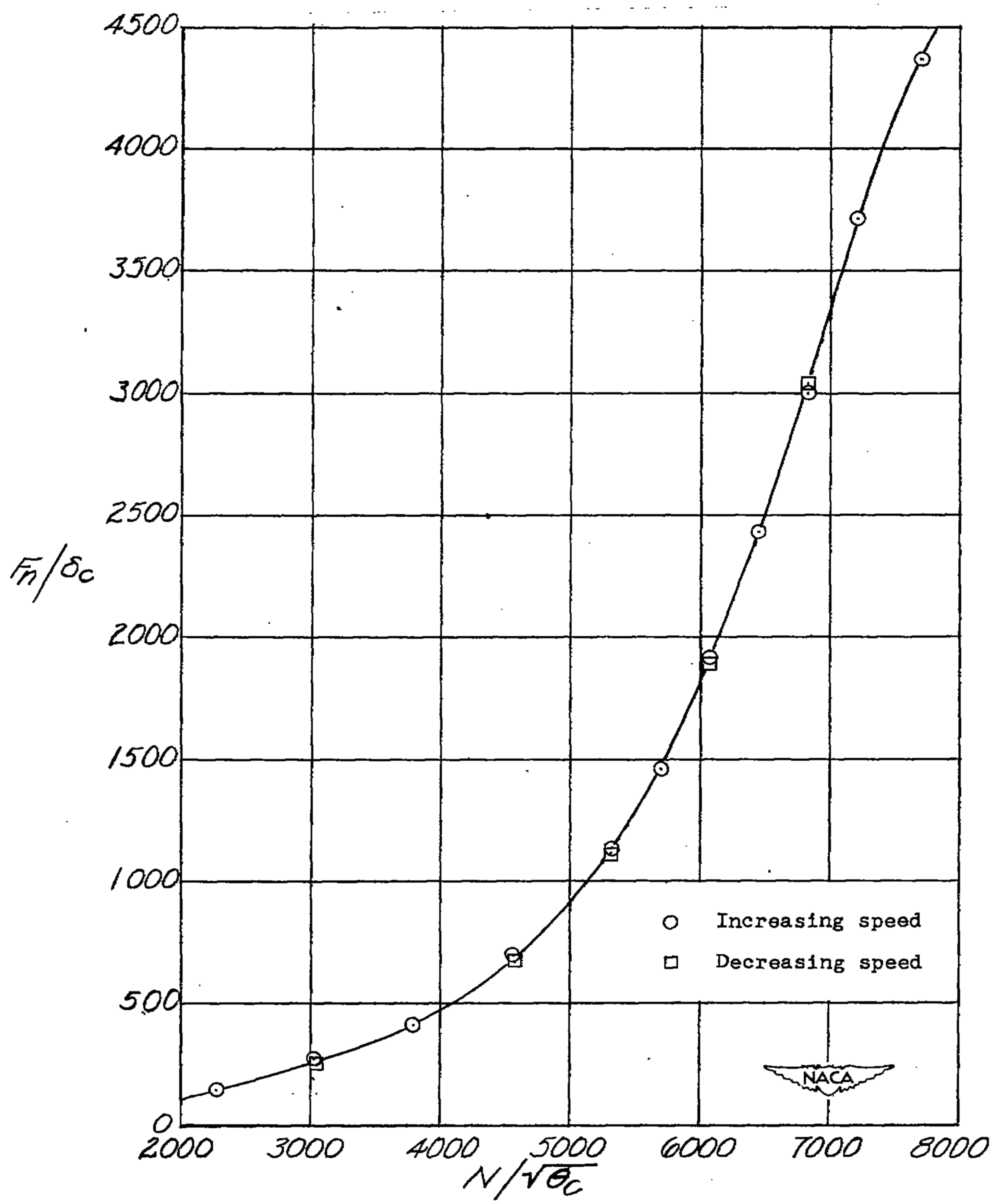

Figure 4.- Variation of normalized engine thrust with normalized engine speed.

3T

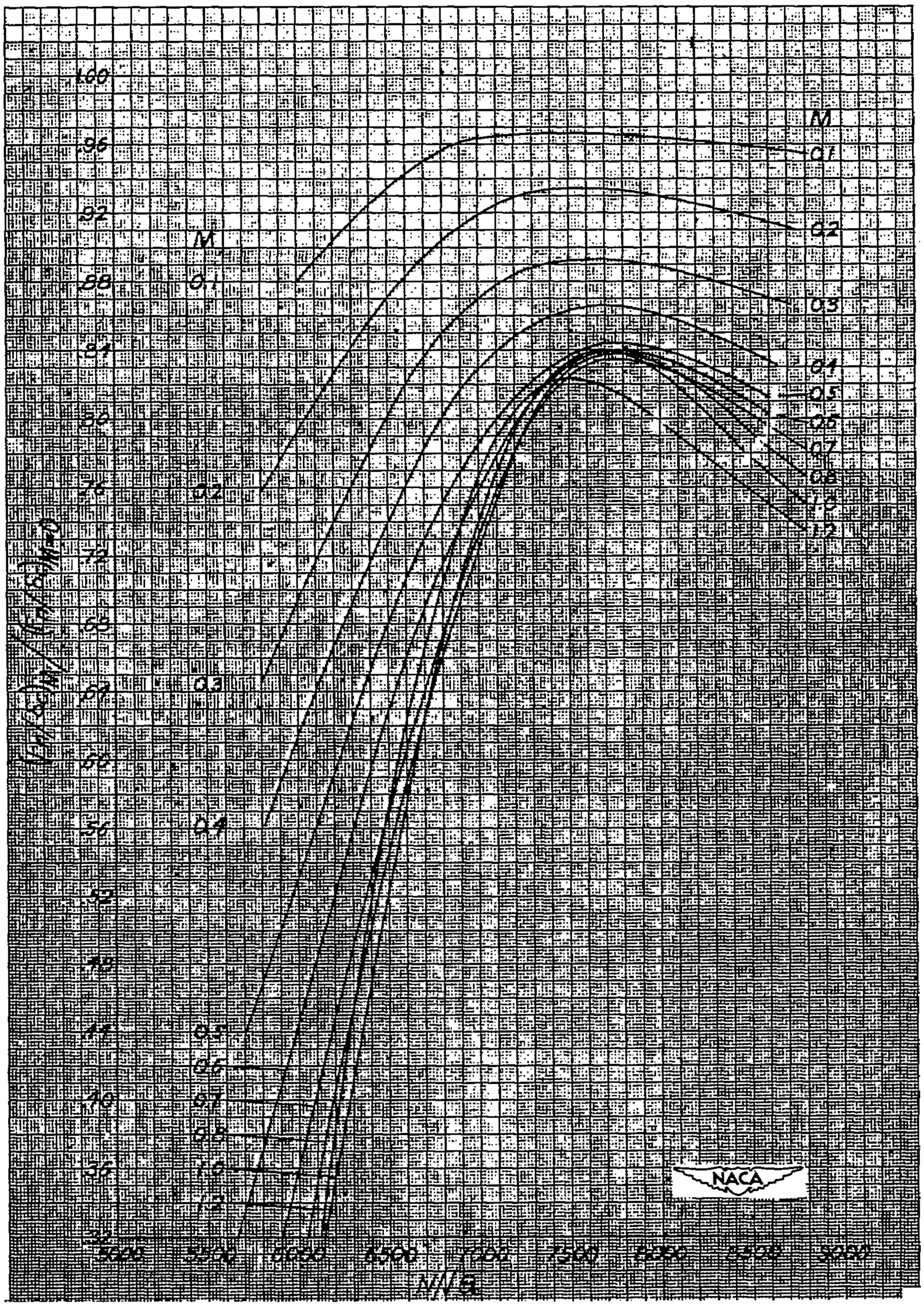

Figure 5.- Factor for correcting engine thrust for various flight Mach numbers.

[redacted]

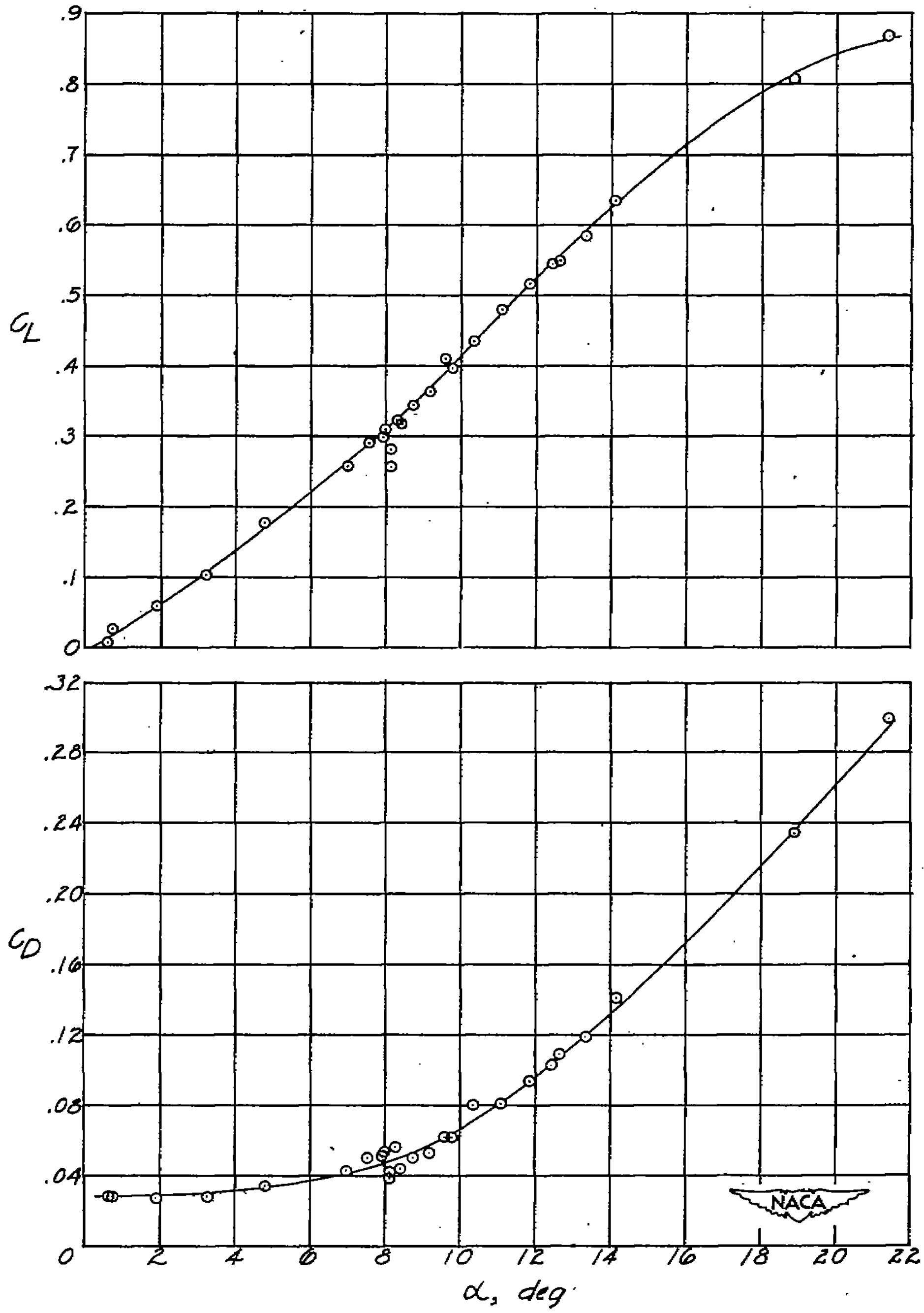

(a) M = 0.60.

Figure 6.- Variation of drag coefficient and lift coefficient with angle of attack for various constant Mach numbers.

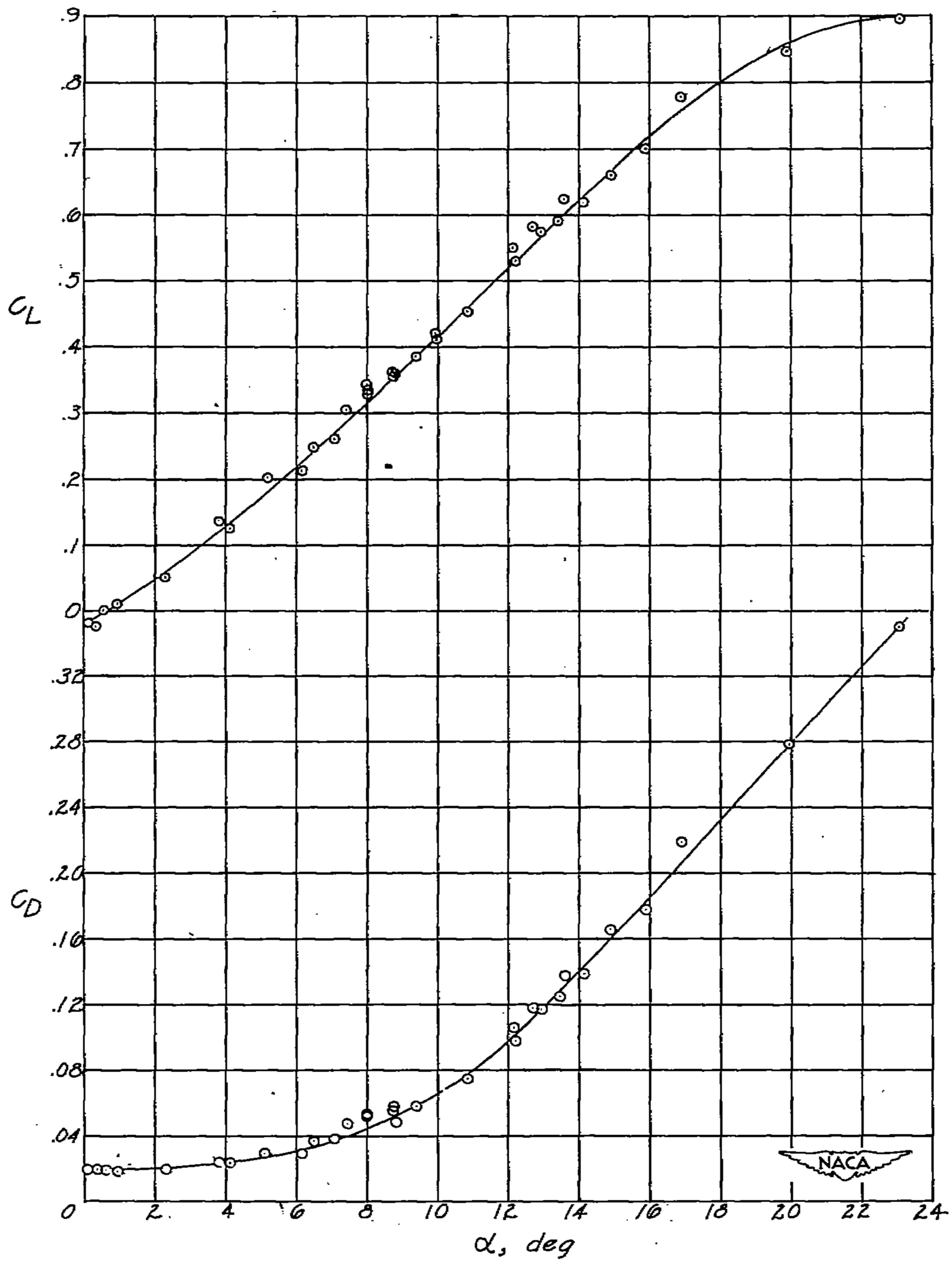

(b) M = 0.70.

Figure 6.- Continued.

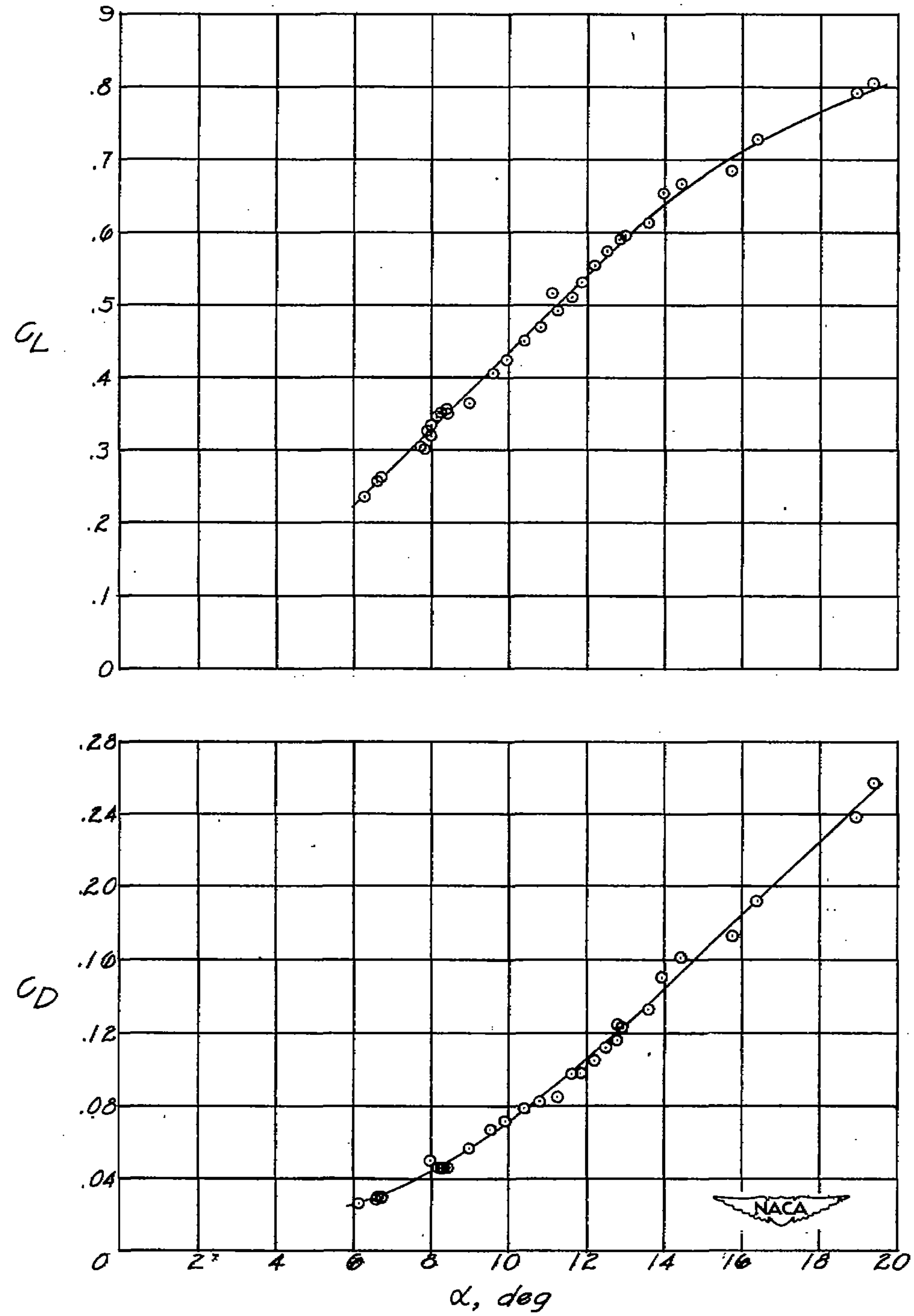

(c) M = 0.75.

Figure 6.- Continued.

[redacted]

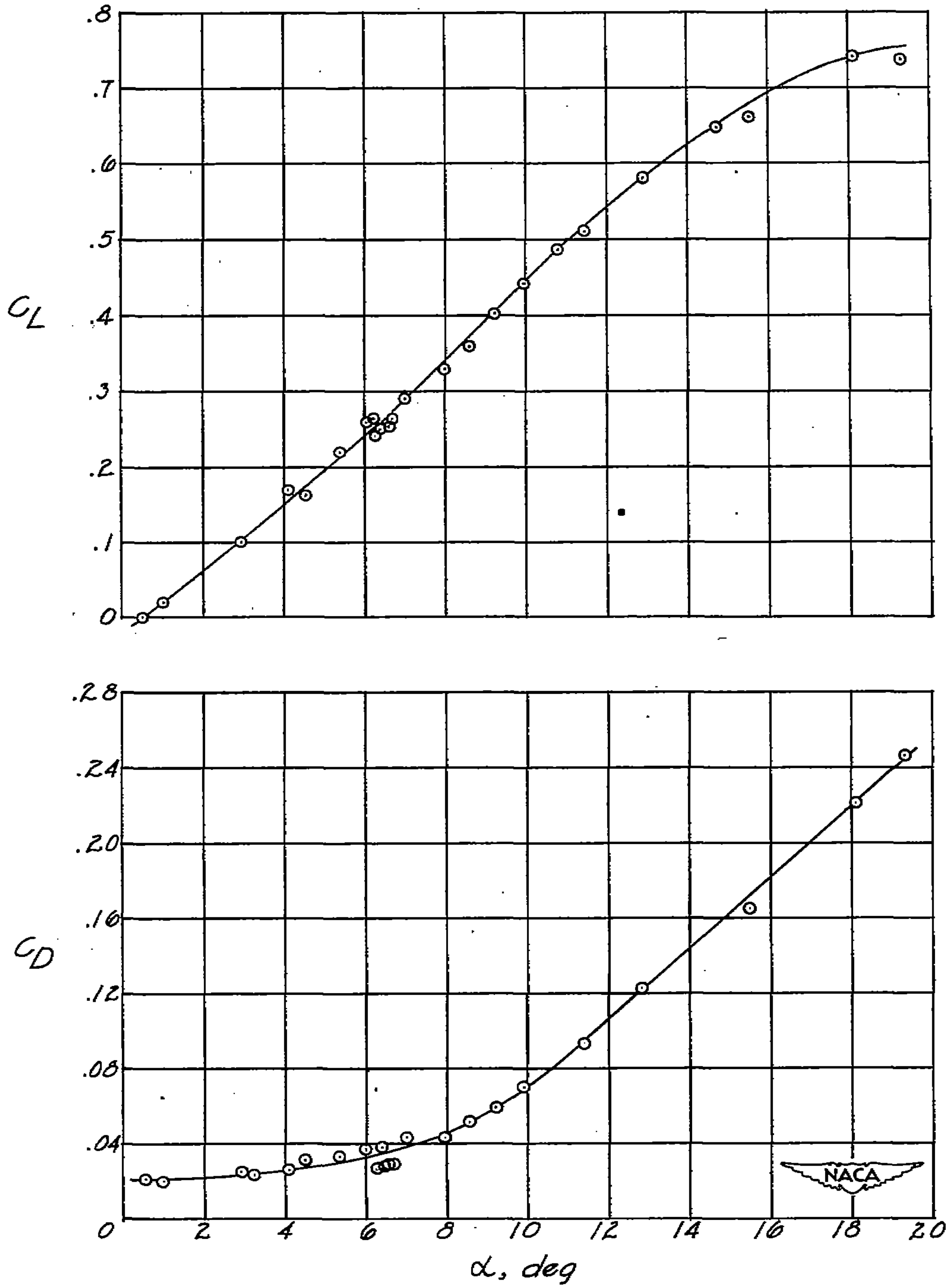

(d) M = 0.80.

Figure 6.- Continued.

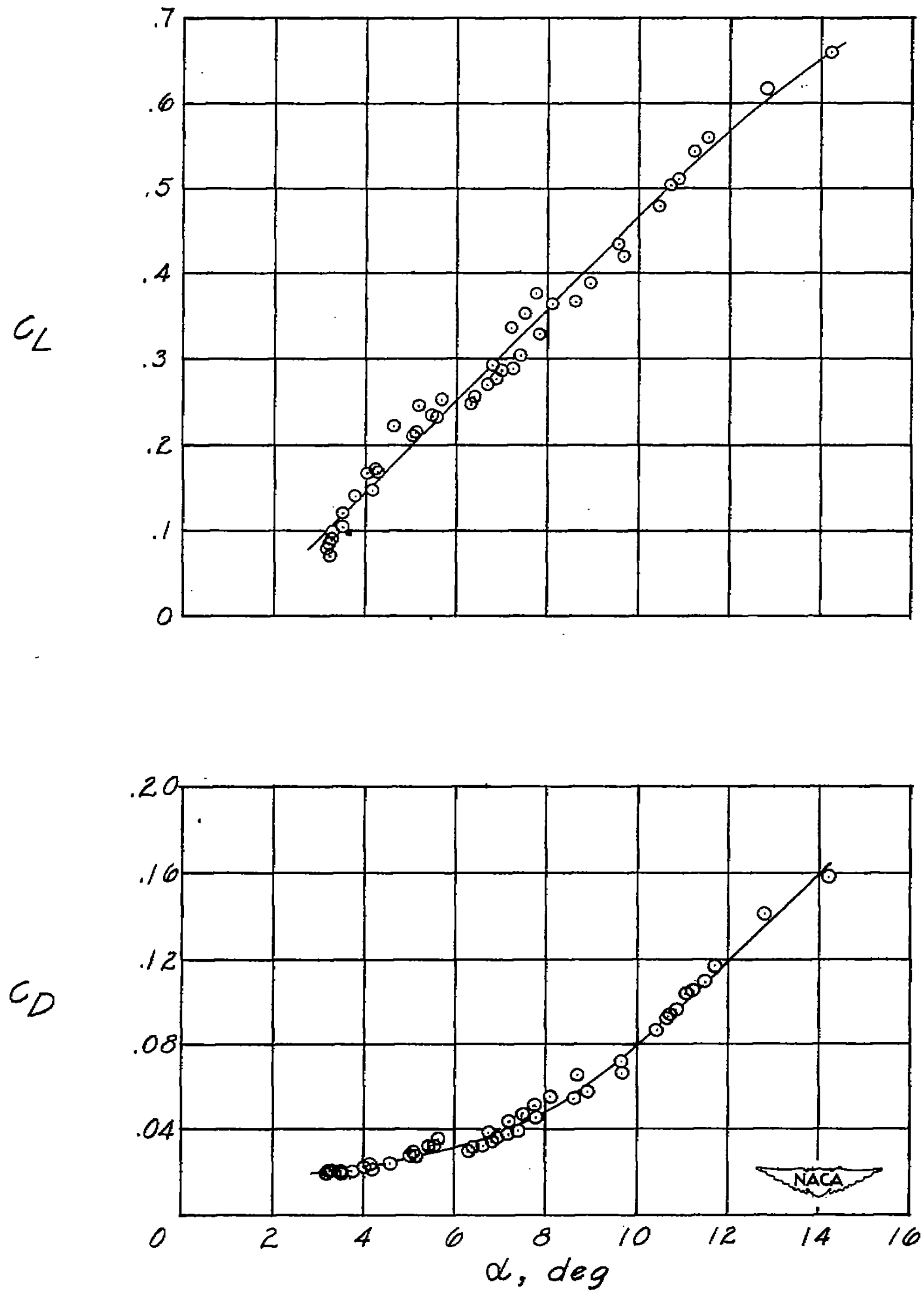

(e) M = 0.84.

Figure 6.- Continued.

[redacted]

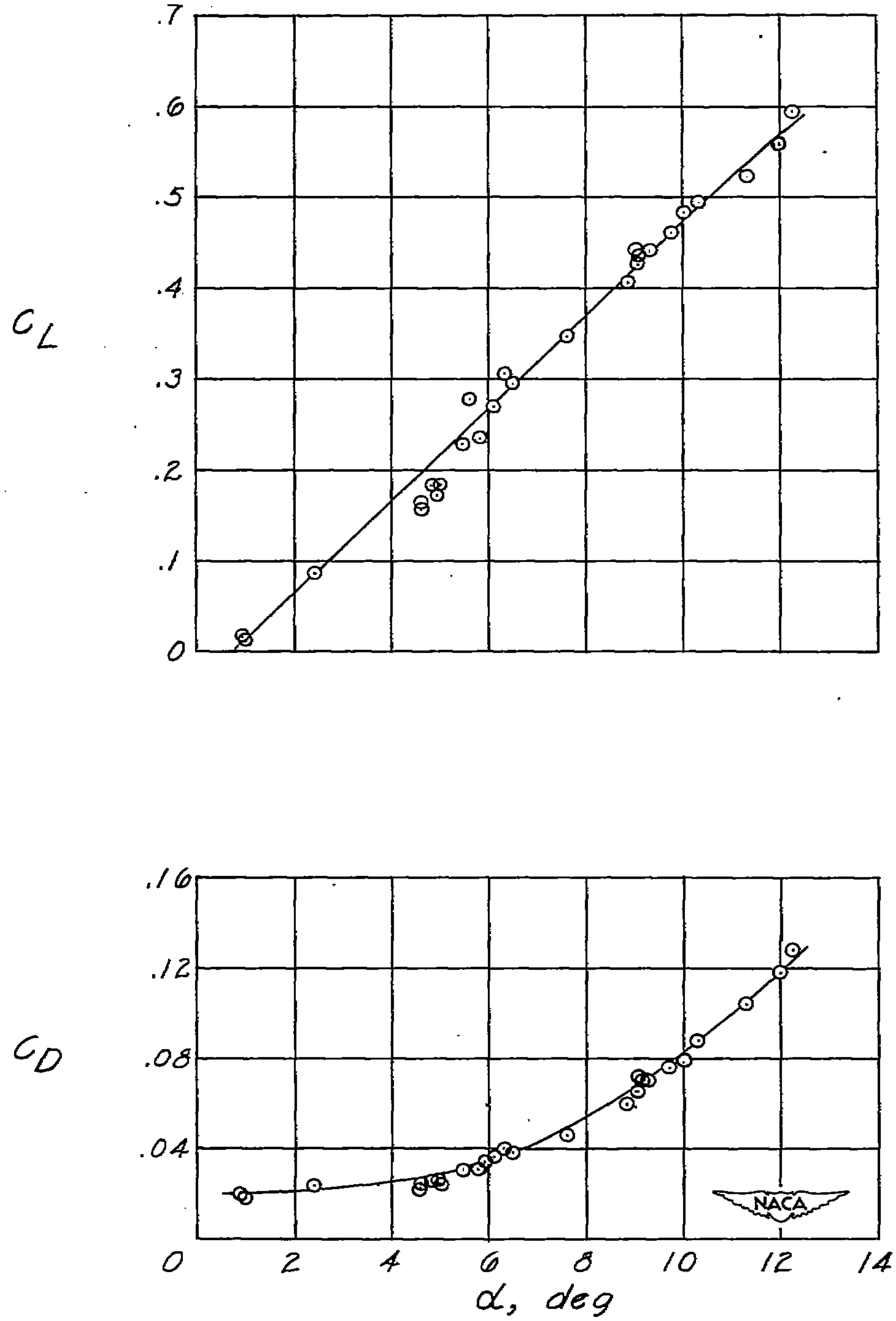

(f) M = 0.88.

Figure 6.- Continued.

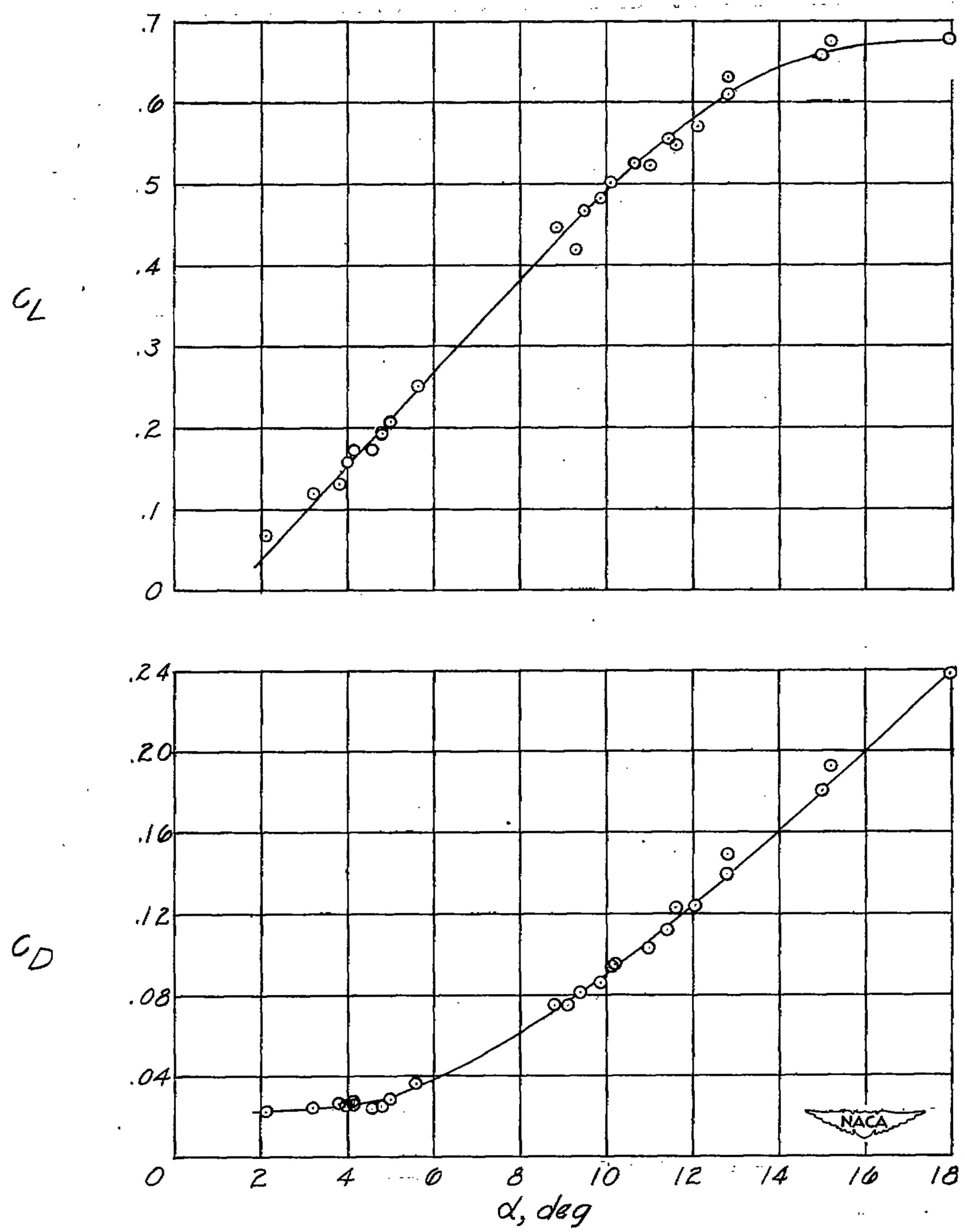

(g) M = 0.90.

Figure 6.- Continued.

[redacted]

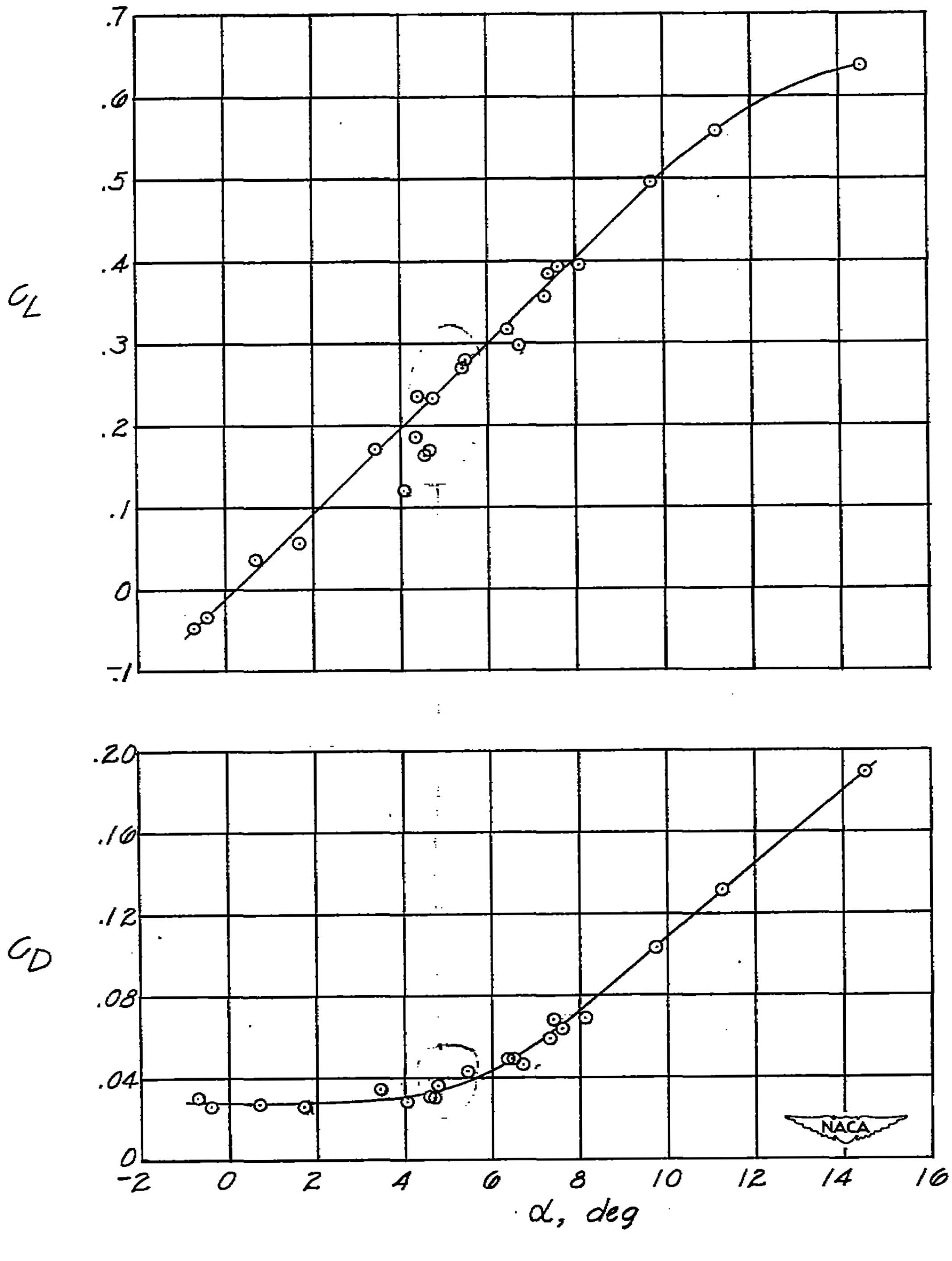

(h) M = 0.93.

Figure 6.- Continued.

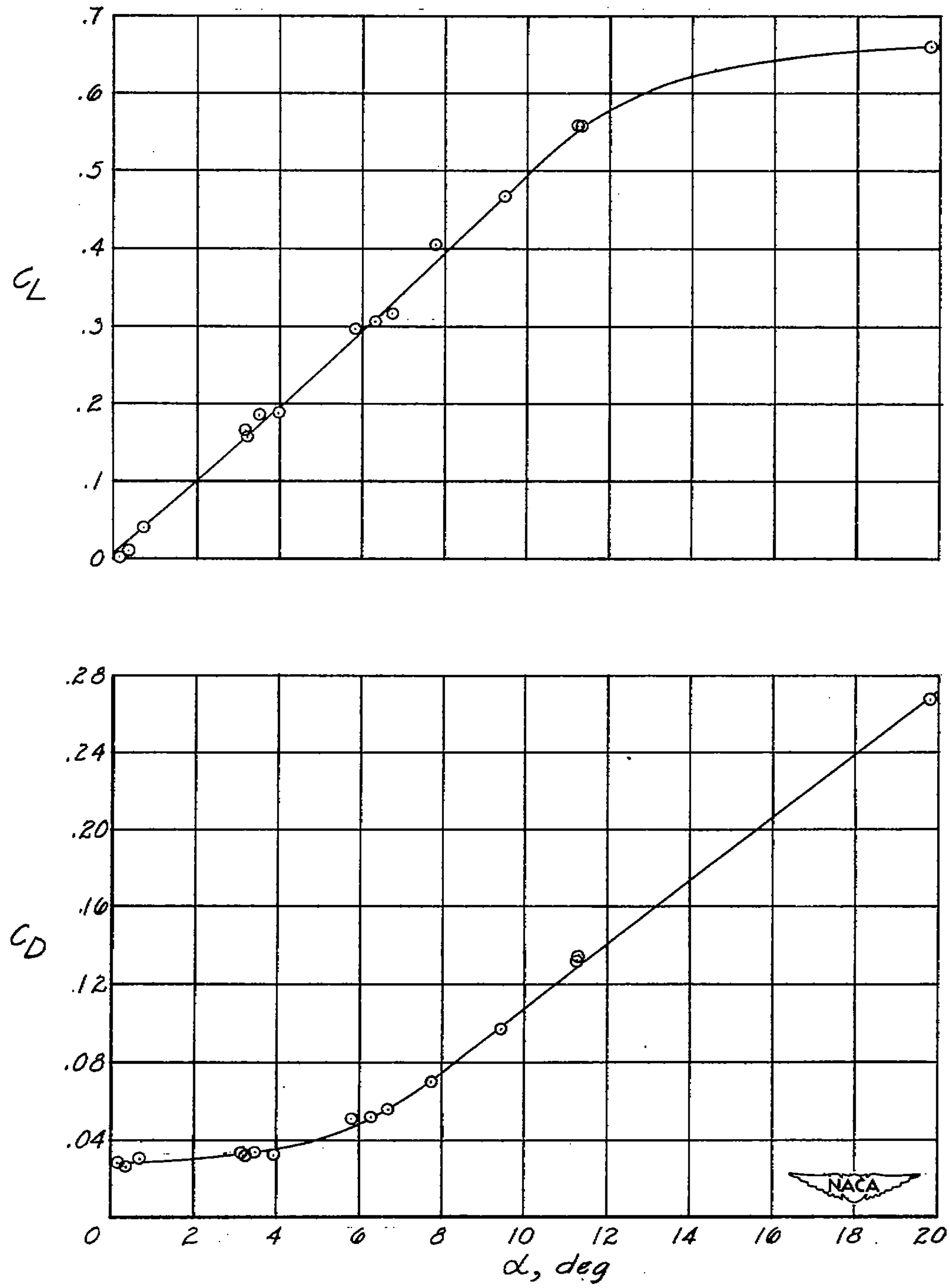

(i) M = 0.94.

Figure 6.- Continued.

[redacted]

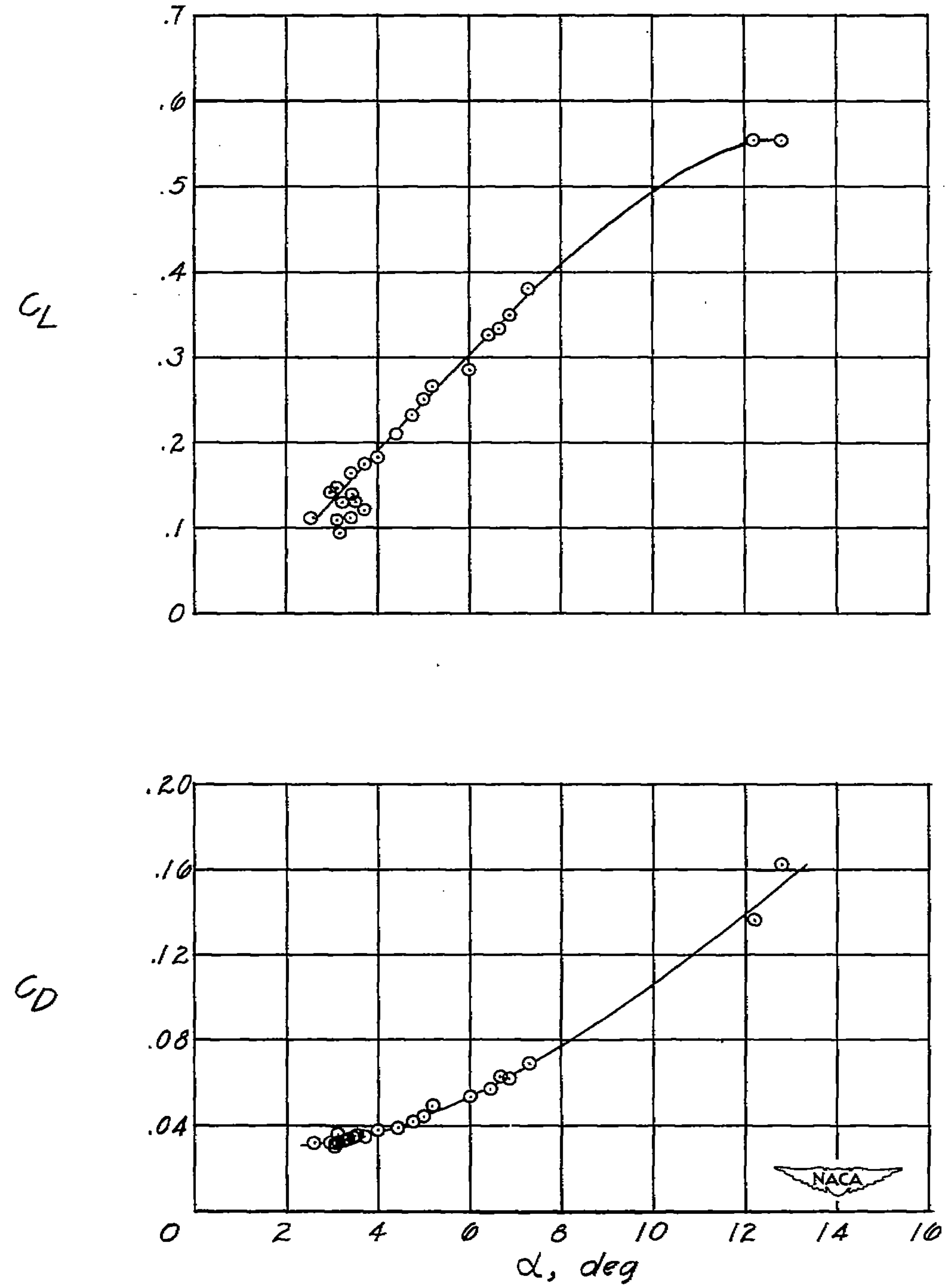

(j) M = 0.95.

Figure 6.- Continued.

[redacted]

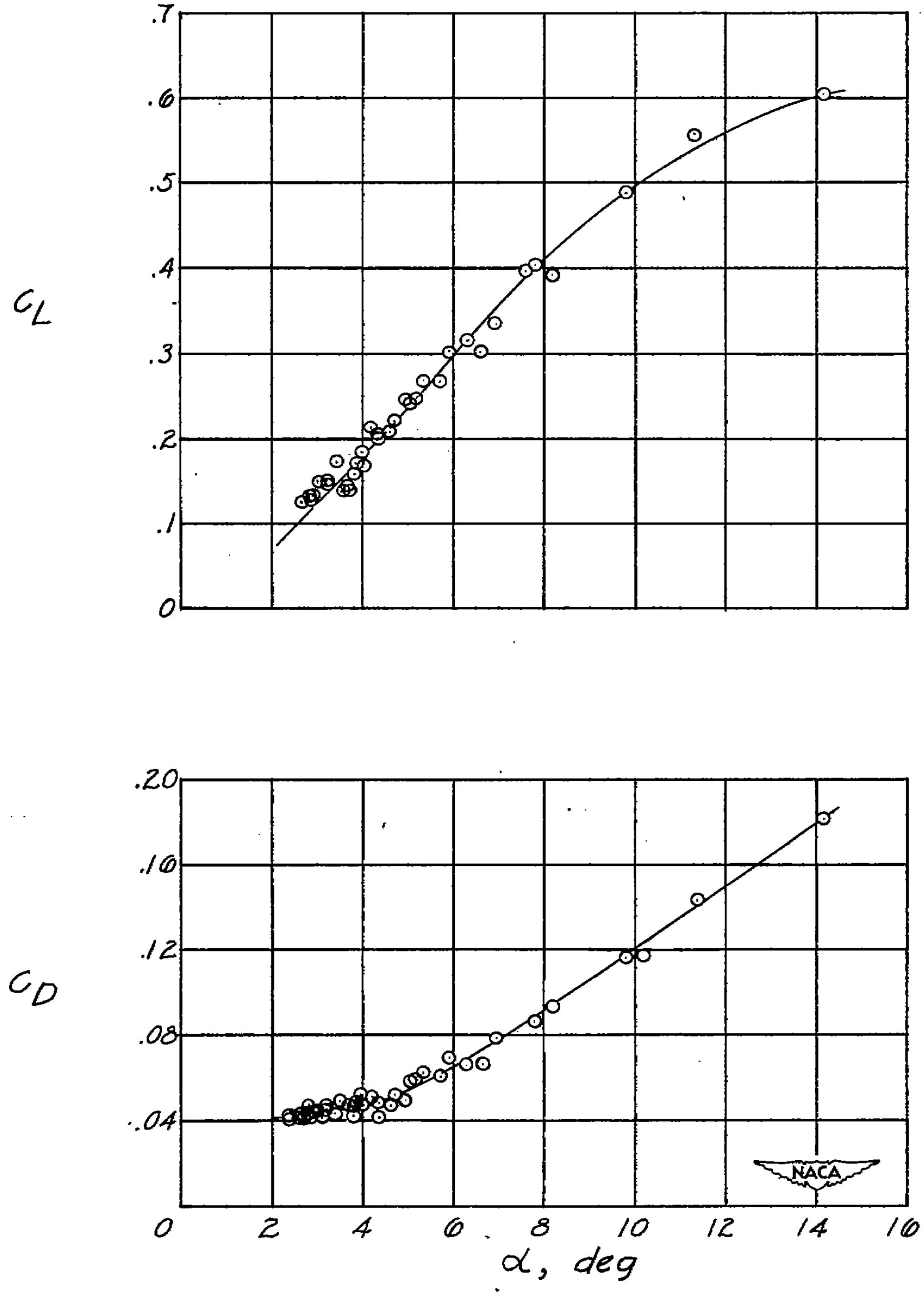

(k) M = 0.96.

Figure 6.- Concluded.

[redacted]

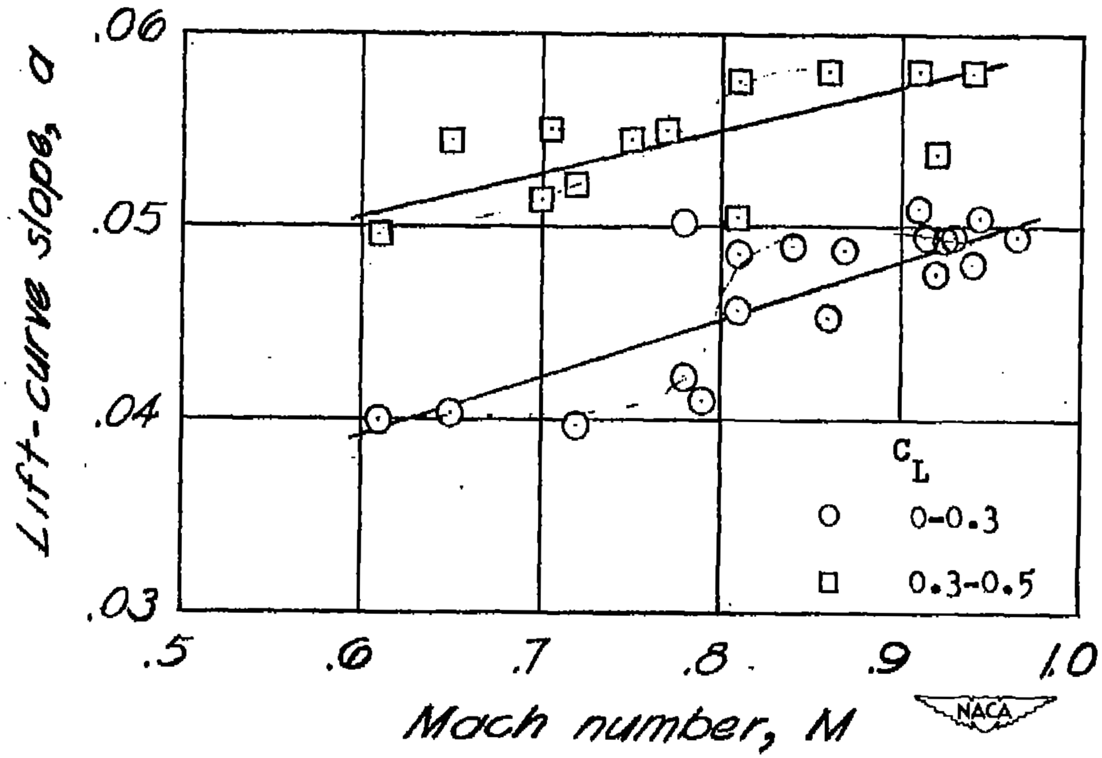

Figure 7.- Variation of lift-curve slope with Mach number.

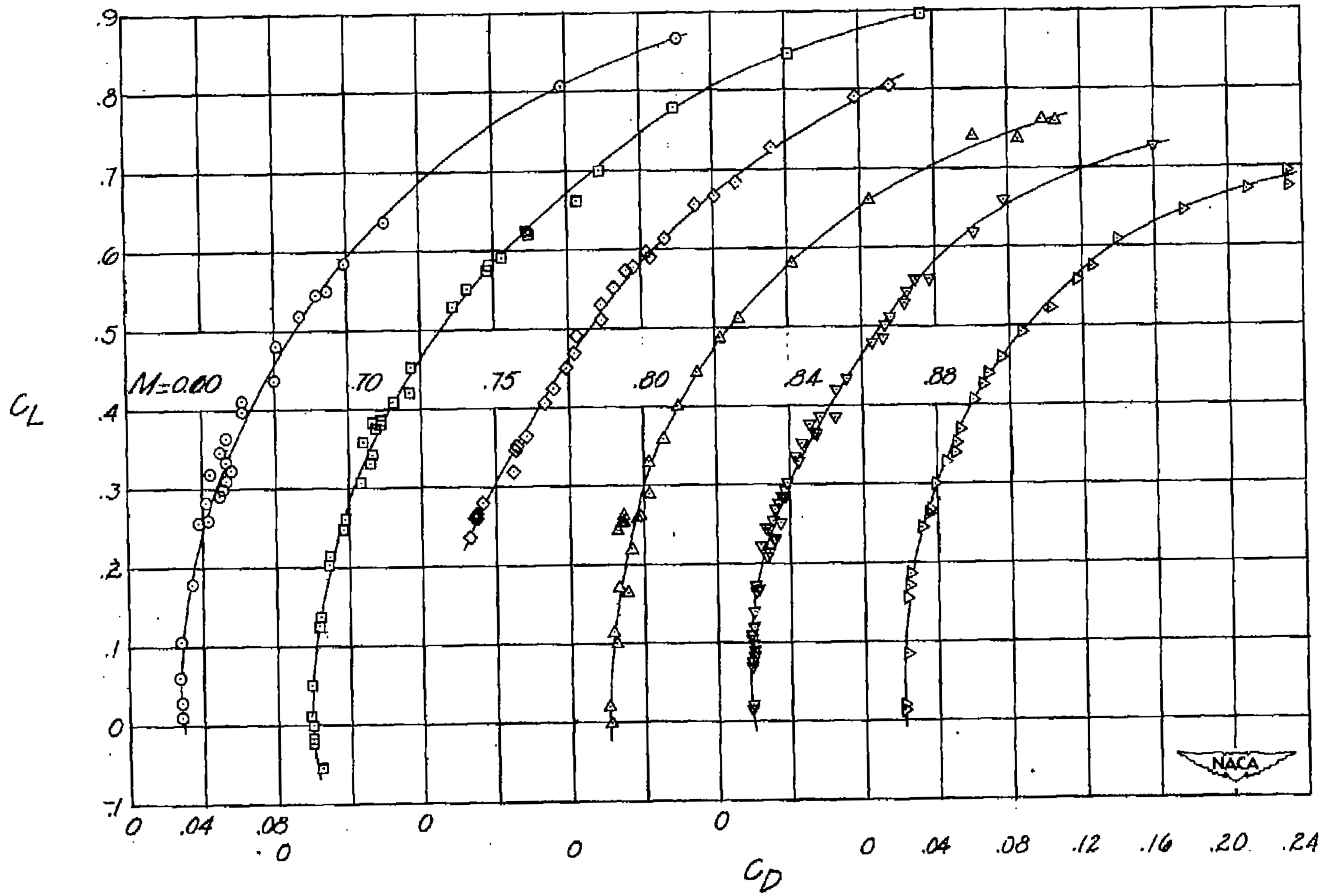

Figure 8.- Variation of drag coefficient with lift coefficient for various constant Mach numbers.

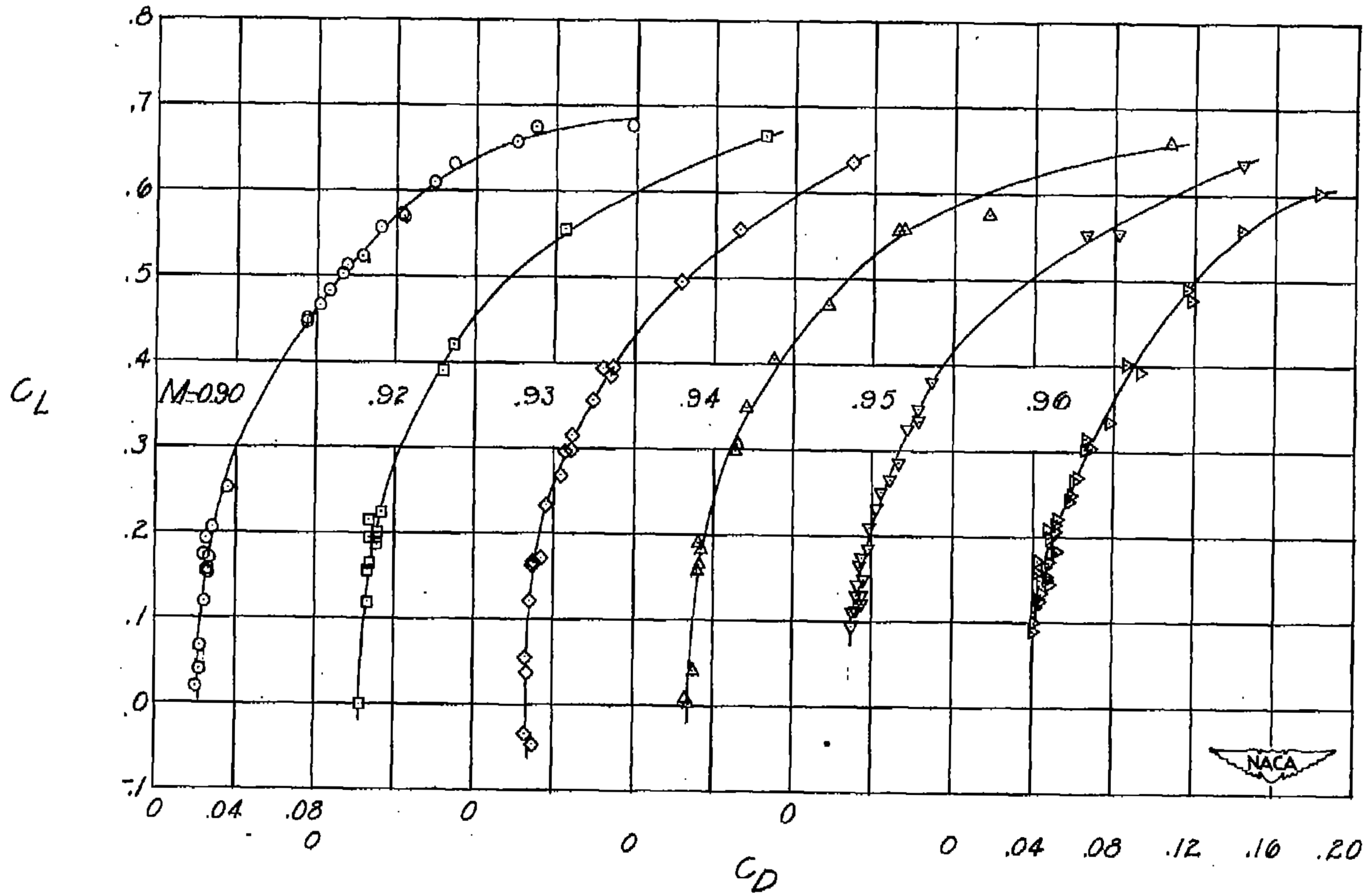

Figure 8.- Continued.

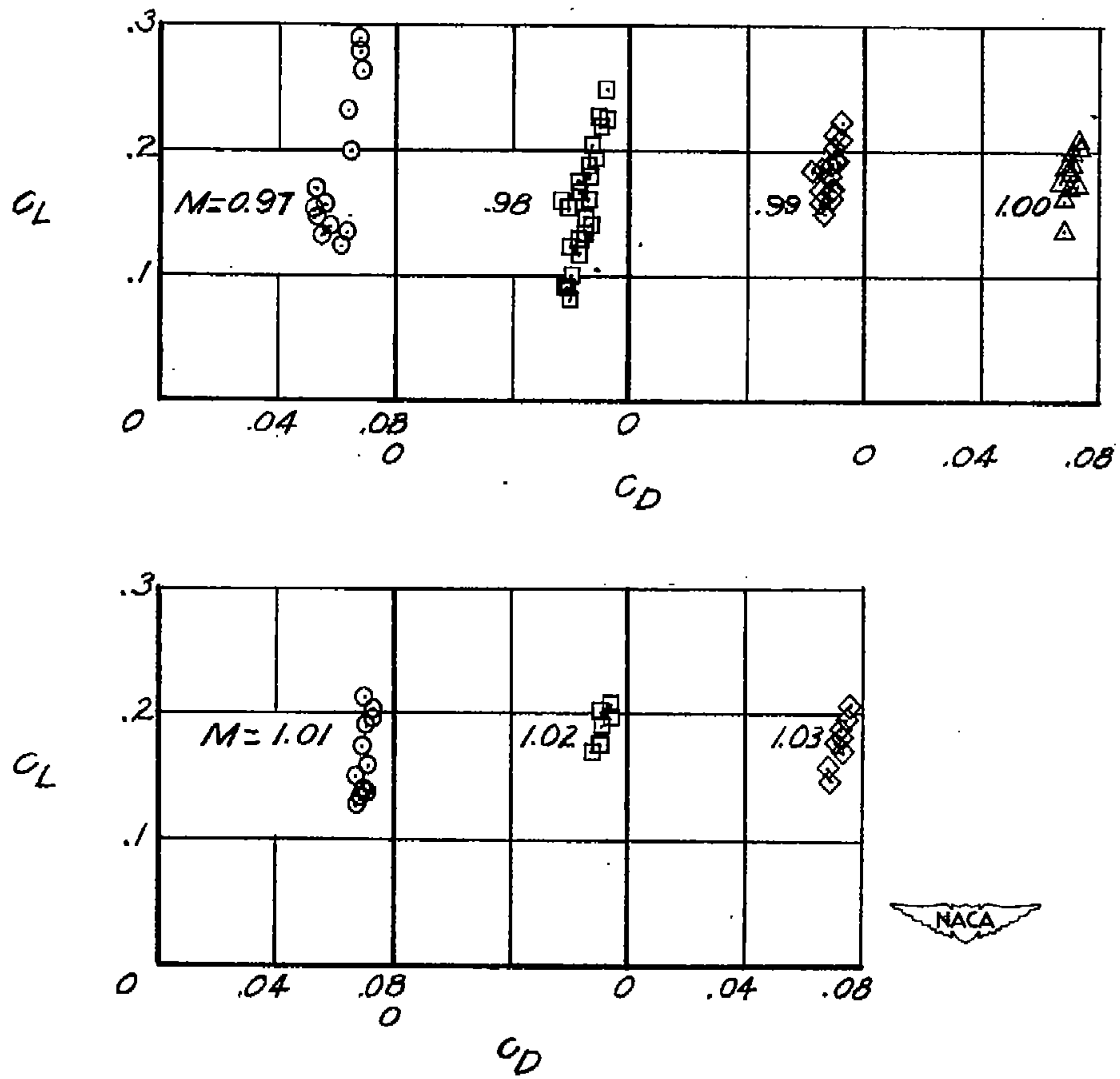

Figure 8.- Concluded.

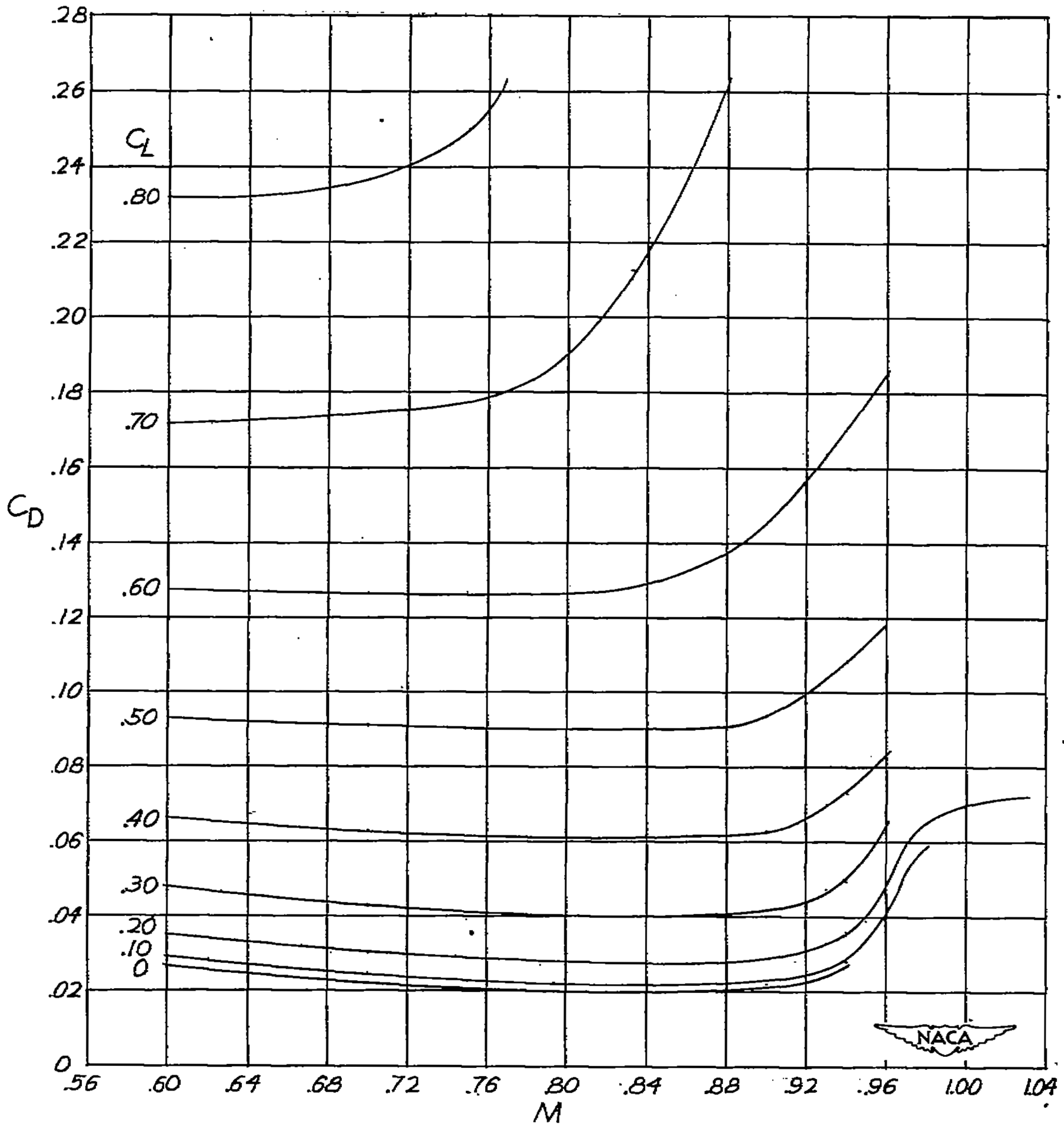

Figure 9.- Variation of drag coefficient with Mach number for various constant lift coefficients.

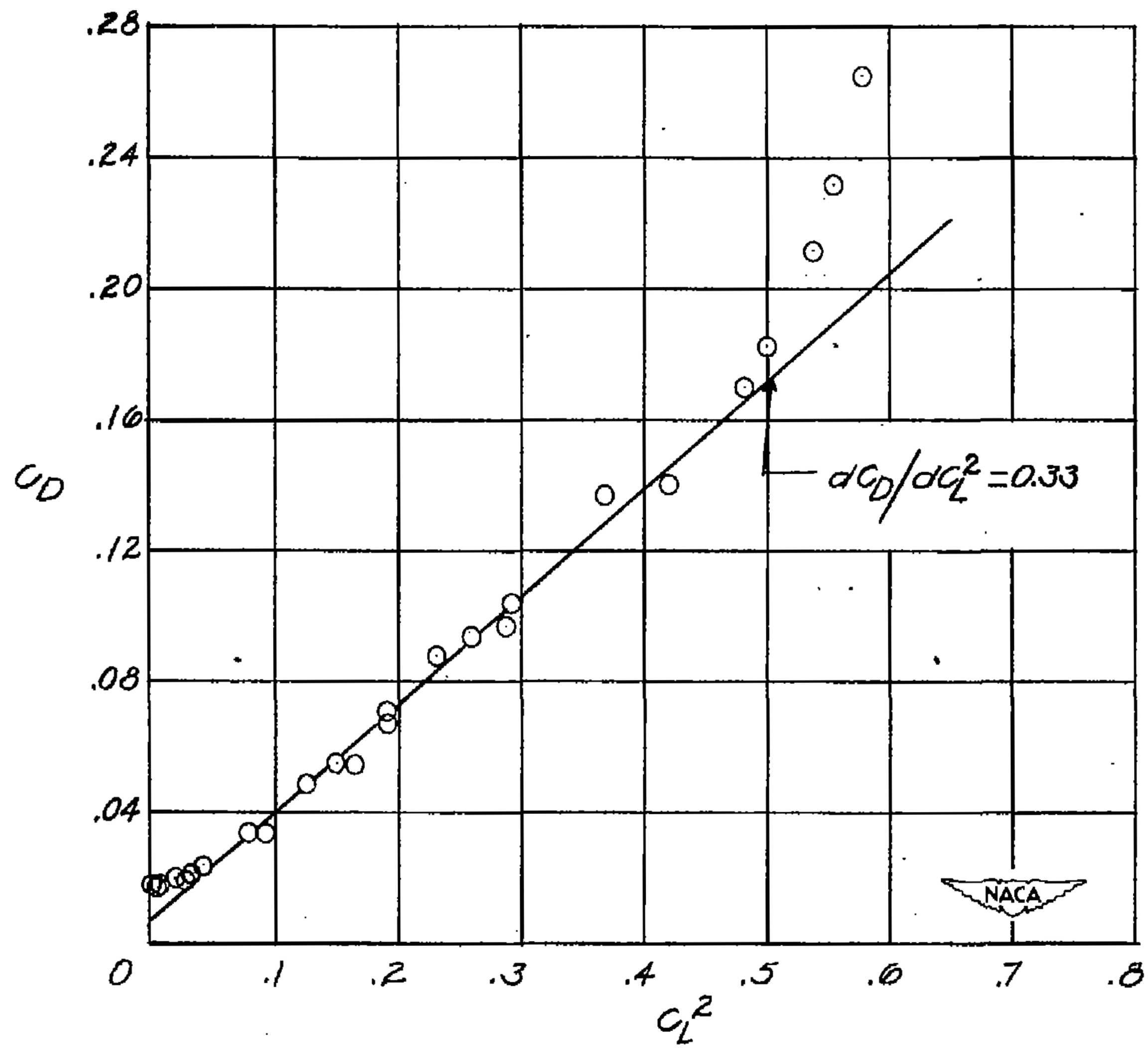

Figure 10.- Typical plot for determination of induced drag factor. M = 0.80.

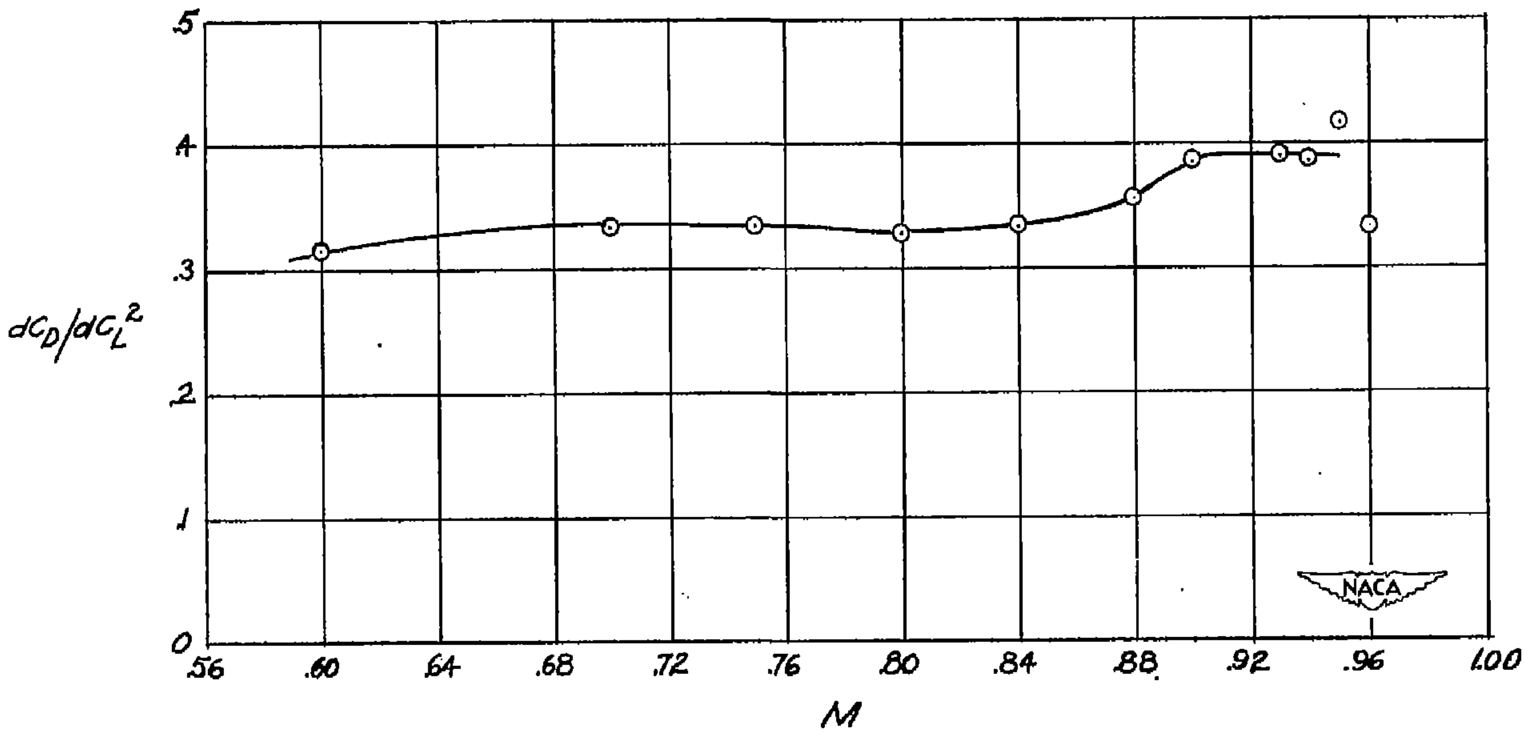

Figure 11.- Variation of induced drag factor with Mach number.
C_L range 0.2 - 0.6.

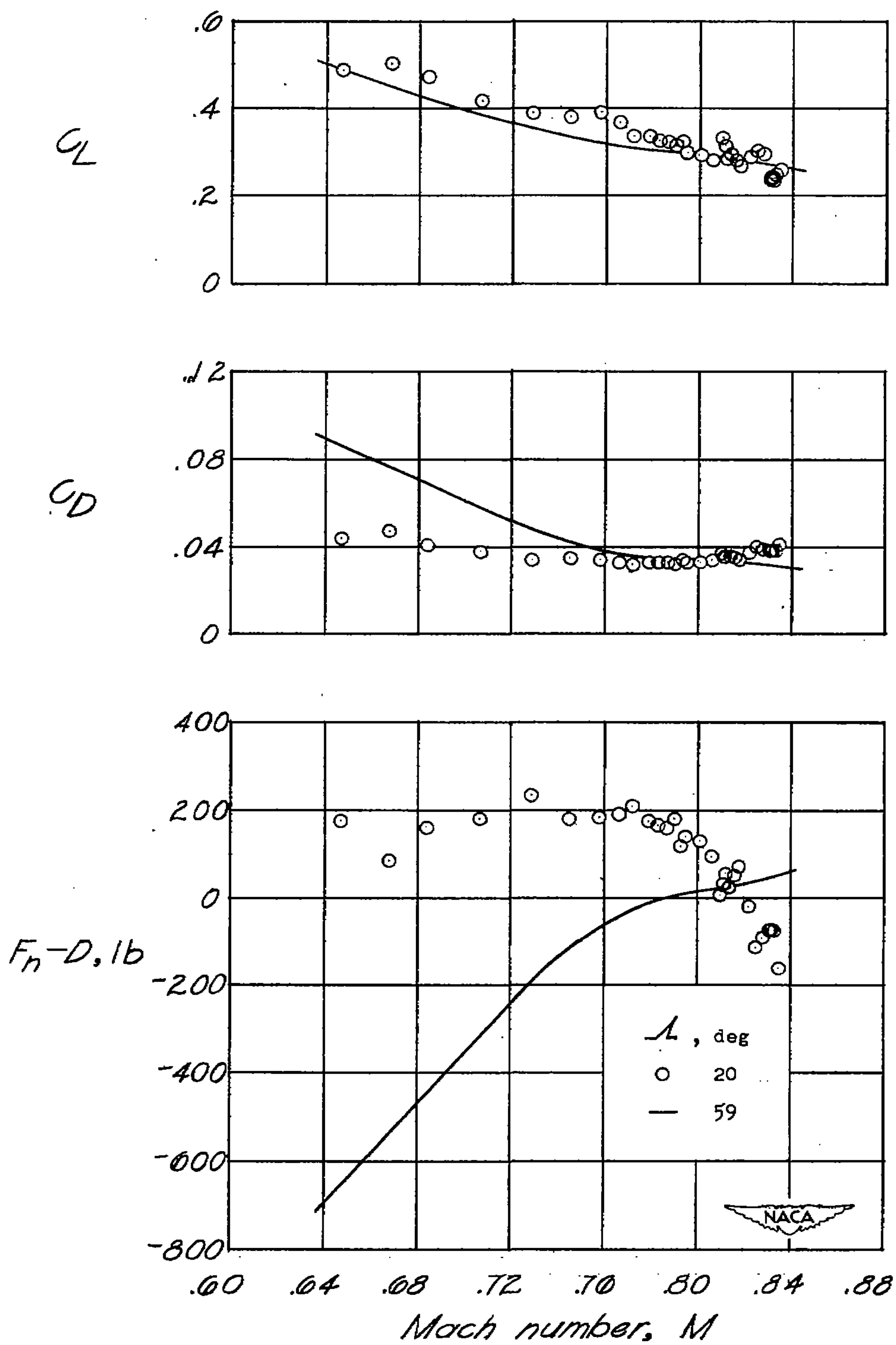

Figure 12.- Comparison of performance of 20° and 59° sweptback configurations in unaccelerated flight at an altitude of about 42,000 feet.

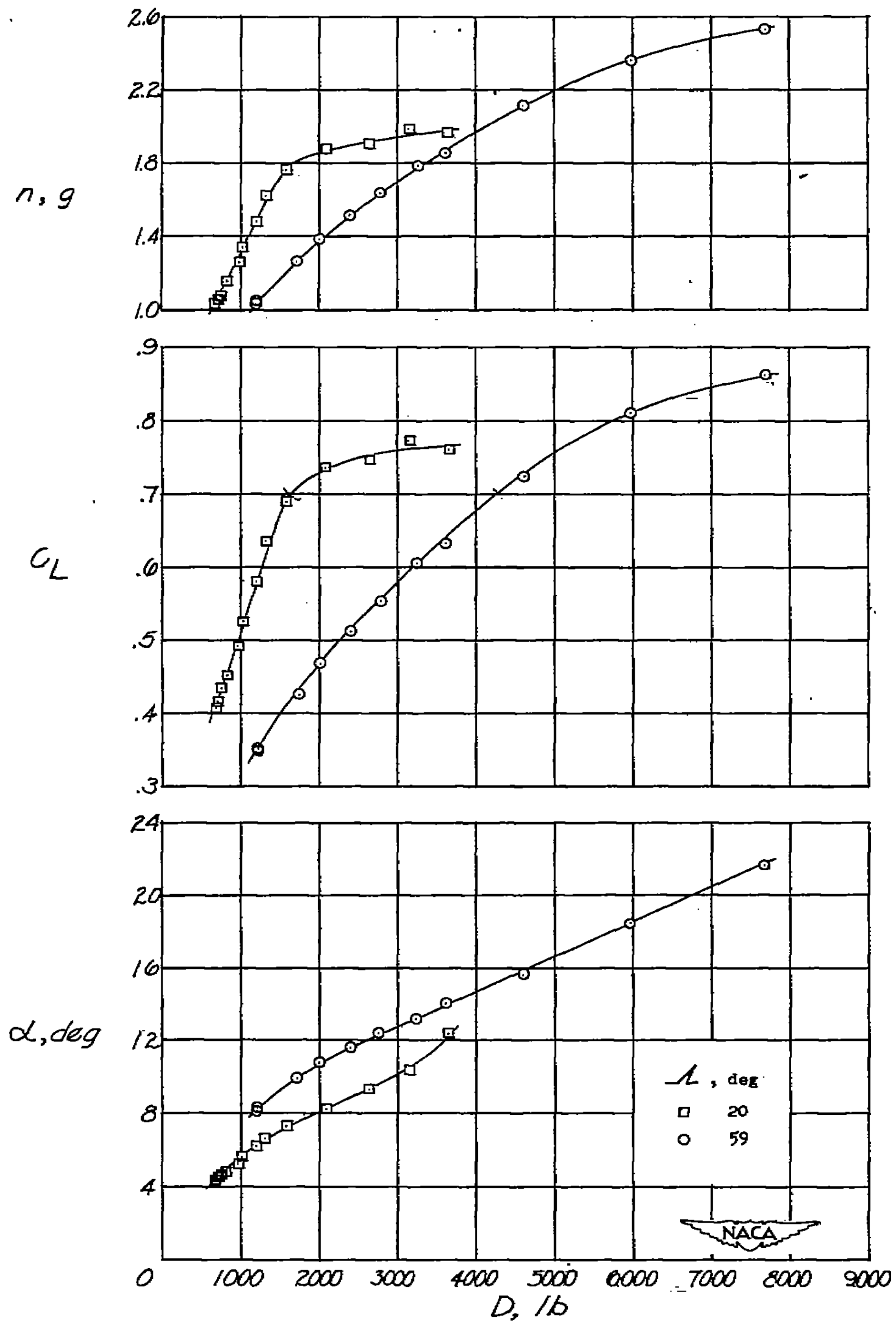

Figure 13.- Comparison of performance of 20° and 59° sweptback configurations in pull-ups at a Mach number of 0.74 and an altitude of 42,000 feet.